

A PULSE CODE MODULATED FIBER OPTIC
LINK DESIGN FOR QUINAULT
UNDER-WATER TRACKING RANGE

David Allen Andersen

NAVAL POSTGRADUATE SCHOOL

Monterey, California



THESIS

A PULSE CODE MODULATED FIBER OPTIC
LINK DESIGN FOR QUINAULT
UNDER-WATER TRACKING RANGE

by

David Allen Andersen

September 1980

Thesis Advisor:

J. P. Powers

Approved for public release; distribution unlimited

0197432

Sc 117610

REPORT DOCUMENTATION PAGE		READ INSTRUCTIONS BEFORE COMPLETING FORM
1. REPORT NUMBER	2. GOVT ACCESSION NO.	3. RECIPIENT'S CATALOG NUMBER
4. TITLE (and Subtitle) A Pulse Code Modulated Fiber Optic Link Design for Quinault Under-Water Tracking Range		5. TYPE OF REPORT & PERIOD COVERED Master's Thesis; September 1980
7. AUTHOR(s) David Allen Andersen		6. PERFORMING ORG. REPORT NUMBER
9. PERFORMING ORGANIZATION NAME AND ADDRESS Naval Postgraduate School Monterey, California 93940		8. CONTRACT OR GRANT NUMBER(s)
11. CONTROLLING OFFICE NAME AND ADDRESS Naval Postgraduate School Monterey, California 93940		10. PROGRAM ELEMENT, PROJECT, TASK AREA & WORK UNIT NUMBERS
14. MONITORING AGENCY NAME & ADDRESS (if different from Controlling Office)		12. REPORT DATE September 1980
		13. NUMBER OF PAGES 90
		15. SECURITY CLASS. (of this report) UNCLASSIFIED
		15a. DECLASSIFICATION/DOWNGRADING SCHEDULE
16. DISTRIBUTION STATEMENT (of this Report) Approved for public release; distribution unlimited		
17. DISTRIBUTION STATEMENT (of the abstract entered in Block 20, if different from Report)		
18. SUPPLEMENTARY NOTES		
19. KEY WORDS (Continue on reverse side if necessary and identify by block number) Fiber Optics, Underwater Communications Link		
20. ABSTRACT (Continue on reverse side if necessary and identify by block number) An underwater fiber optics communication link has been shown to be a realistic alternative to the currently planned coaxial cable link for the shallow-water torpedo tracking range at the Naval Undersea Warfare Engineering Station. The currently planned system is reviewed in this thesis and a fiber optic alternative is discussed. Several possible modulation techniques are studied and compared. Choosing pulse code modulation, a fiber optic link was built and tested using a microprocessor controlled signal simulator. A		

discussion of this link; including signal formal, optical transmission and reception is included. Fiber optic communications in general is an emerging field with new concepts and active research. Several of these concepts are discussed and their possible integration into a fiber optic shallow-water torpedo tracking range is suggested.

Approved for public release; distribution unlimited

A Pulse Code Modulated Fiber Optic Link
Design for Quinault Under-Water Tracking Range

by

David Allen Andersen
Lieutenant, United States Coast Guard
B.S., United States Coast Guard Academy, 1973

Submitted in partial fulfillment of the
requirements for the degree of

MASTER OF SCIENCE IN ELECTRICAL ENGINEERING

from the

NAVAL POSTGRADUATE SCHOOL
September 1980

ABSTRACT

An underwater fiber optics communication link has been shown to be a realistic alternative to the currently planned coaxial cable link for the shallow-water torpedo tracking range at the Naval Undersea Warfare Engineering Station. The currently planned system is reviewed in this thesis and a fiber optic alternative is discussed. Several possible modulation techniques are studied and compared. Choosing pulse code modulation, a fiber optic link was built and tested using a microprocessor controlled signal simulator. A discussion of this link; including signal format, optical transmission and reception is included. Fiber optic communications in general is an emerging field with new concepts and active research. Several of these concepts are discussed and their possible integration into a fiber optic shallow-water torpedo tracking range is suggested.

TABLE OF CONTENTS

I.	INTRODUCTION- - - - -	6
A.	DESCRIPTION OF CURRENT PLANNED SYSTEM - - - -	7
B.	FIBER OPTIC ALTERNATIVE- - - - -	10
C.	FIBER OPTICS - AN EMERGING FIELD- - - - -	12
II.	PROPOSED SYSTEM - - - - -	26
A.	OVERALL DESCRIPTION AND BLOCK DIAGRAM - - - -	26
B.	SIGNAL SIMULATOR- - - - -	28
C.	SIGNAL MODULATION - - - - -	34
D.	OPTICAL TRANSMITTER - - - - -	46
E.	FIBER LINK- - - - -	56
F.	OPTICAL RECEIVER- - - - -	63
G.	SIGNAL DEMODULATOR- - - - -	67
H.	SIGNAL POWER BUDGET AND DISPERSION CALCULATIONS- - - - -	74
III.	CONCLUSIONS AND RECOMMENDATIONS - - - - -	82
	LIST OF REFERENCES- - - - -	86
	INITIAL DISTRIBUTION LIST - - - - -	89

I. INTRODUCTION

The field of optical communications is widely viewed as a new technology, however, in 1880 Alexander Graham Bell invented and patented a light-wave communications device, the Photophone. The light beam was acoustically modulated, transmitted through the atmosphere and demodulated using a selenium detector [1]. Atmospheric absorption and scattering presented a fundamental problem, the solution ultimately being the optical waveguide. Today, one hundred years since Bell first communicated on light beams, optical fiber communications is one of the fastest growing areas of modern electronics for a variety of reasons.

One potential application of this expanding technology is undersea communication links, specifically an underwater torpedo tracking range at the Naval Undersea Warfare Engineering Station, Keyport, Washington. Earlier works relating to this application have shown the feasibility and viability of a fiber optic link [2, 3]. The purpose of this work is to discuss some previously unmentioned advantages of an optical fiber communications system for the shallow-water range at Keyport and to present some new concepts being actively researched. Several possible modulation schemes are discussed and compared. Finally, one system is proposed and documented.

A. CURRENTLY PLANNED SYSTEM

Current plans for the shallow-water torpedo tracking range at Keyport, Washington are tentative and any information in this section must be viewed in that light. The shallow-water range referred to as the Quinault Under-water Tracking Range (QUTR) will be located in the open ocean. All other tracking ranges at Keyport, Washington are in protected waters. The layout of QUTR is represented in Figure 1. As a torpedo passes through the tracking range it emits a signal which is picked up by the array of hydrophones. The signal contains identification and telemetry information which is transmitted over coaxial cable from each hydrophone to a multiplexer and then on to the shore facility at Kalalock, Washington. From there, the information is conditioned and transmitted over a microwave link to the Pacific Beach Tracking and Control Center for final processing.

The modulation scheme to be used for QUTR is Spaced Frequency Shift Keying (SFSK). This is identical to normal frequency shift keying except that there is a space or dead-time between each different frequency signal as shown in Figure 2. Because of the shallow-water and highly reflective sandy bottom, a serious multipath problem exists. The space between frequency transmission allows for some of this signal echo to attenuate before another tone burst is sent,

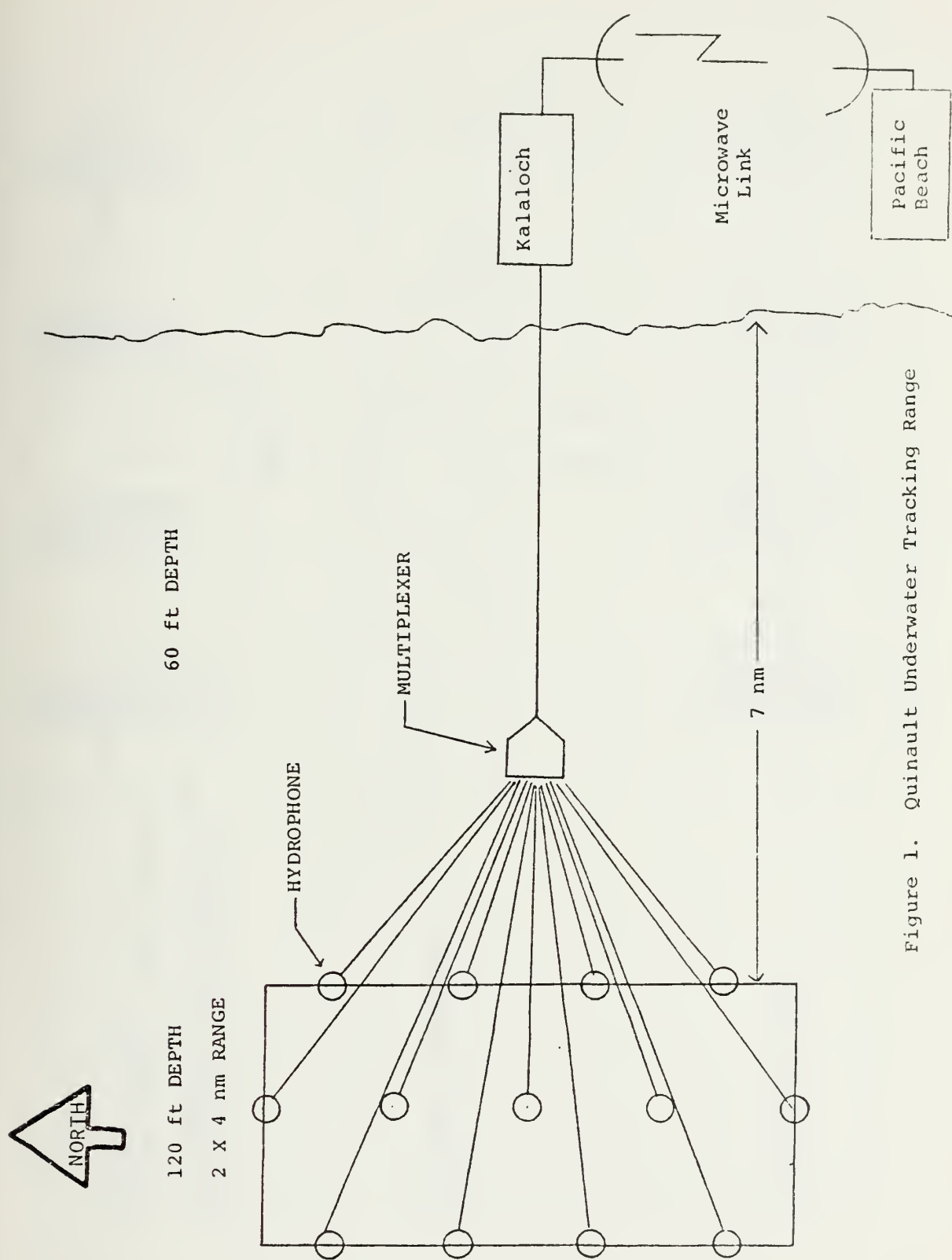
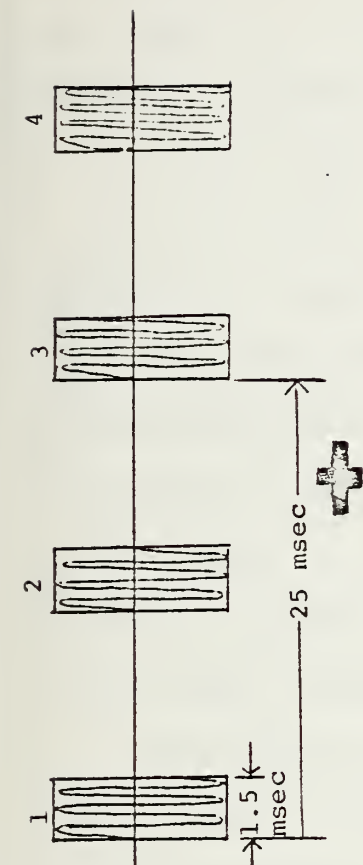
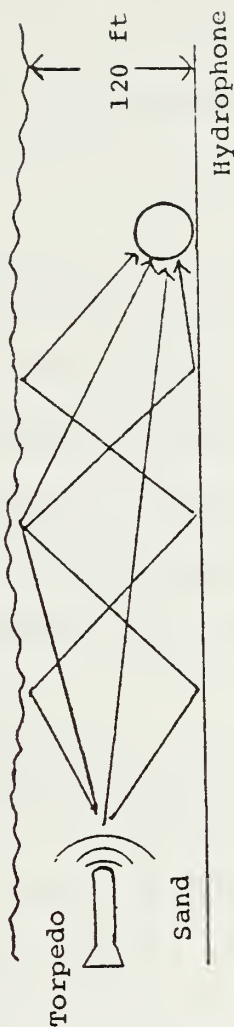


Figure 1. Quinault Underwater Tracking Range

TORPEDO SIGNAL
 SPACED FREQUENCY SHIFT KEYING
 ODD NUMBERED BITS: IDENTIFICATION
 EVEN NUMBERED BITS: TELEMETRY



MULTIPATH INTERFERENCE



HYDROPHONE SIGNAL

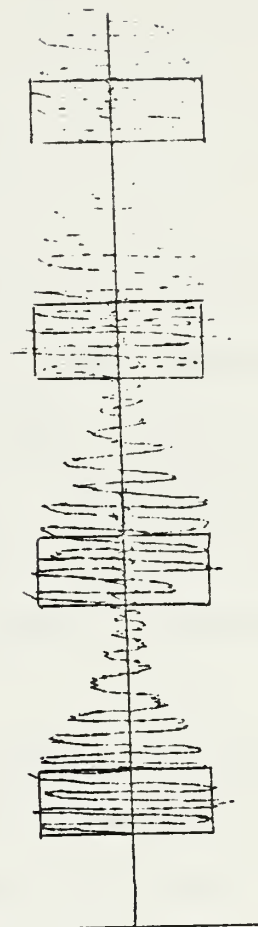


Figure 2. Signal Format

as shown in Figure 2. Since the information is contained in the frequency of the signal and not the amplitude, attenuation is not a concern. The speed of a torpedo varies and can range up to 60 knots. At the higher speeds, the Doppler shift in frequency must be accounted for:

$$\Delta f = \frac{vf}{c} \quad (1)$$

where Δf is Doppler shift, v is relative velocity, f is the operating frequency and c is the speed of light. Although this Doppler shift seems to be a disadvantage it may be used to recover a component of torpedo velocity. The QUTR frequency bands are shown in Figure 3. Bands 1 and 2 accommodate high speed torpedos while Band 3 is used for tracking a low speed torpedo.

QUTR will be located in the Pacific Ocean. Therefore, the range will experience higher sea states than those in protected waters. Also, the cable to shore will have to pass through the surf zone.

B. FIBER OPTIC ALTERNATIVE

Commercial fiber optic systems for telephone communications have been proven in an operational status now for about three years. Today's development efforts are not concentrating on making fiber optic communications work, but rather improving them with new technology. For this reason, a fiber optic system proposed for installation

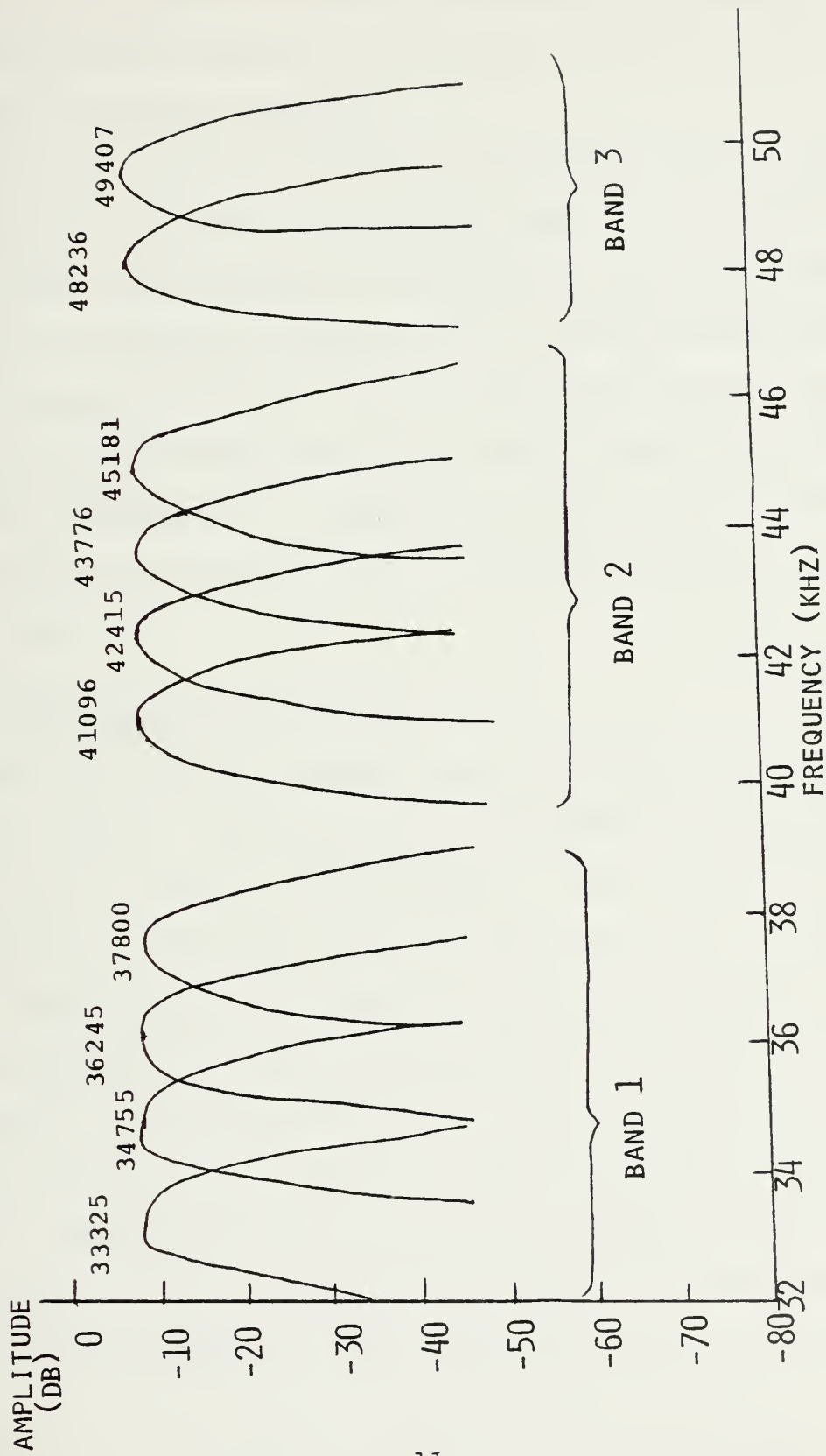


Figure 3. Tracking Frequency Bands (SFSK)

today for QUTR will be different than one proposed for installation several years in the future. Fortunately, a system installed today could be added to and improved upon without a complete redesign.

Initially the link from the multiplexer to Kalaloch, see Figure 1, could be an optical fiber cable. Then the links from the individual hydrophones to the multiplexers could be connected to fiber cable. Current trends indicate that optical multiplexers are a future possibility and several research groups are even doing studies on fiber optical hydrophones. A complete fiber optic system from hydrophone to microwave link may be realizable in the next five years.

C. FIBER OPTICS-AN EMERGING FIELD

Man has employed optical means in communications since ancient times. Early Greek writers refer to visual signaling such as flag and smoke signals. The Navy began experimenting with flashing light in the 1800's [4]. During the last twenty years technological advances have led to the construction of large-bandwidth optical information-transfer systems. The development of the laser and light emitting diode in the sixties began the rapid evolution of fiber optic communication. Once waves at optical frequencies were generated, a low loss transmission medium and sensitive receiver were needed. These needs were filled during the

seventies with the production of the first low-loss fiber optics transmission link and the invention and development of silicon PIN and avalanche photodiode detectors.

Today, the essential ingredient in each fiber optic system is the crucial utilization of one or more of the five attractive features of optical fibers: low-loss, wide bandwidth, small crosssection, light weight, and non-inductive property. These advantages have been developed and related to the QUTR elsewhere [2, 3] and consequently will not be discussed here. The optical fiber is not just a replacement of coaxial cable; rather it performs what the coaxial cable could do poorly or simply could not do. Consequently, the disadvantages of new technology (e.g., short history, possible unknown factors, inexperience) count little. Currently the cost of fiber optic cable is about equal to that of coaxial cable. The future will bring nothing but higher copper costs and, as technology and demand increase, lower fiber optic costs.

The fact that fiber optics is a relatively new field can be viewed as an advantage. New concepts and active research are continually increasing the potential of such systems. To design for the future, it is important to recognize the current and projected potential of fiber optic cable systems. To aid in this effort, some new and novel concepts in fiber optics will be presented.

One trend very evident in the technology today is the move towards longer wavelengths of operation. This is primarily to achieve the lower attenuation levels possible there. Attenuation losses in fibers are due to several phenomena which often operate simultaneously:

1. Absorption losses are primarily due to OH^- ions and certain transition metal ions which have electronic transitions in the wavelength range of interest and which cause absorption of bands. High silica waveguides are regularly made in which the metal ions do not contribute to the loss. The only impurity for which a direct correlation has been made is the OH radical, whose bands at 725, 825, 875 and 950 nanometers are clearly visible in Figure 4. The strength of the 950 nanometers band has been shown to be approximately 1 dB/km/ppm [5]. All absorption in the spectrum shown can be accounted for by OH^- absorption. It can be seen that absorption decreases at certain higher wavelengths (above 1 micron).

2. Scattering loss in state-of-the-art low-loss fibers is attributed primarily to scattering centers in the fibers. These may be due to inhomogeneities frozen into the glass during the drawing process or more importantly, the result of intrinsic inhomogeneities of the material. This intrinsic scattering is believed to represent the fundamental limit to attenuation in waveguides [5]. This loss, α_s , can be calculated as follows:

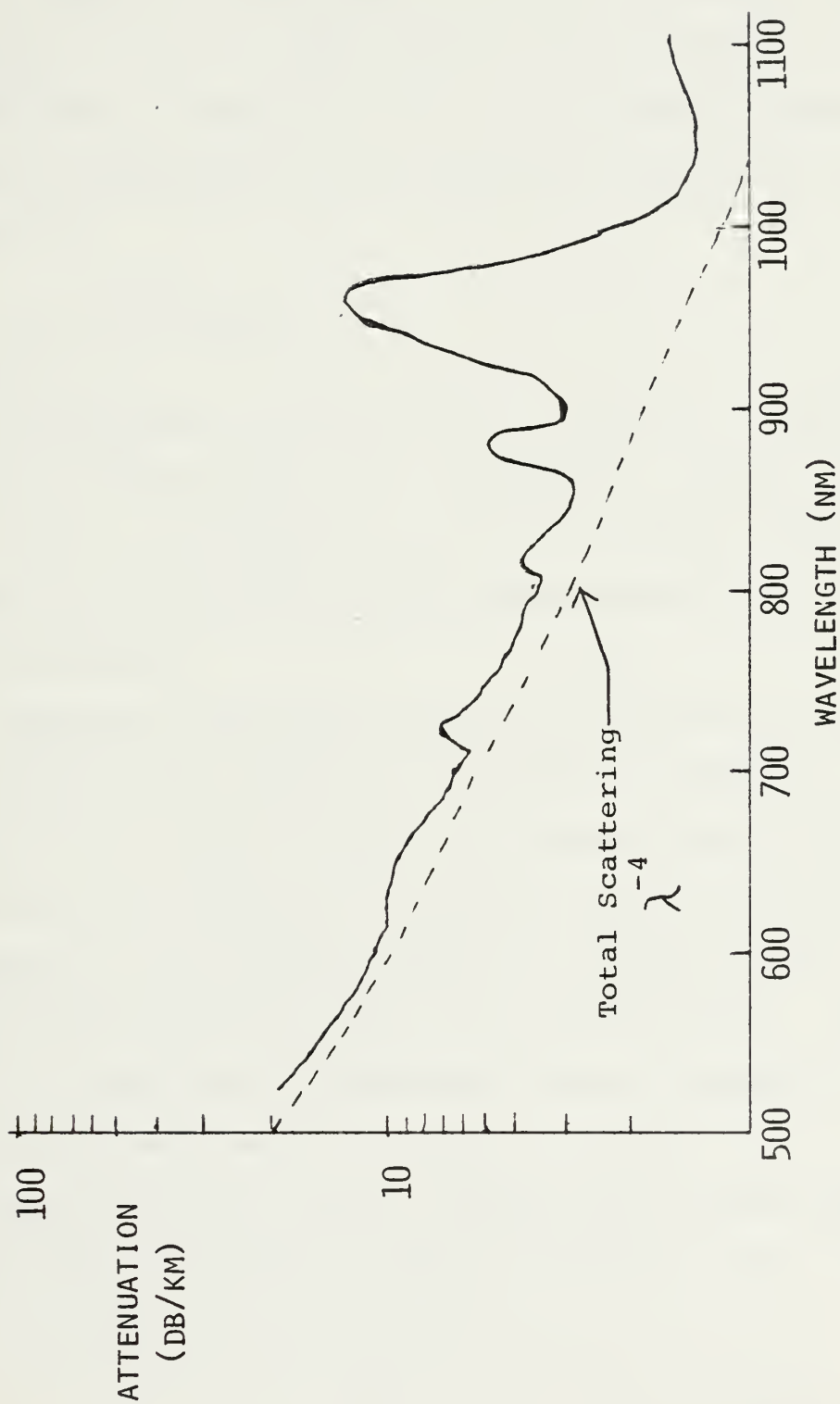


Figure 4. Attenuation Spectrum for a High Silica Waveguide

$$\alpha_s = \frac{8\pi^3}{3\lambda^4} (n^2 - 1) k T \beta \quad (2)$$

where T is the transition temperature at which the fluctuations are frozen into the glass, β is the isothermal compressibility, λ is the wavelength of the transmitted light, n is the index of refraction and k is Boltzmann's constant [6]. Using present day silica materials, Equation (2) can be reduced to

$$\alpha_s = R \lambda^{-4} \text{ dB/km} \quad (3)$$

where λ is expressed in microns and the constant R takes the value of 1.5 dB/km·micron [7]. Equation (3) clearly shows that it will be advantageous to move to a longer operating wavelength as long as the material absorption loss is small at that wavelength.

3. Radiation losses are caused by the bending of fibers, particularly at small radii of curvature, or geometric irregularities in the optical fiber and imperfections at the core to cladding interface. A special type of bending called microbending can be created during the cabling process. It is caused by microscopic bumps in the cabling media. These losses are independent of wavelength and are generally negligible for bend radii in excess of ~10 cm.

Attenuation losses decrease dramatically as wavelength increases above 1 micron as shown in Figure 5. For λ

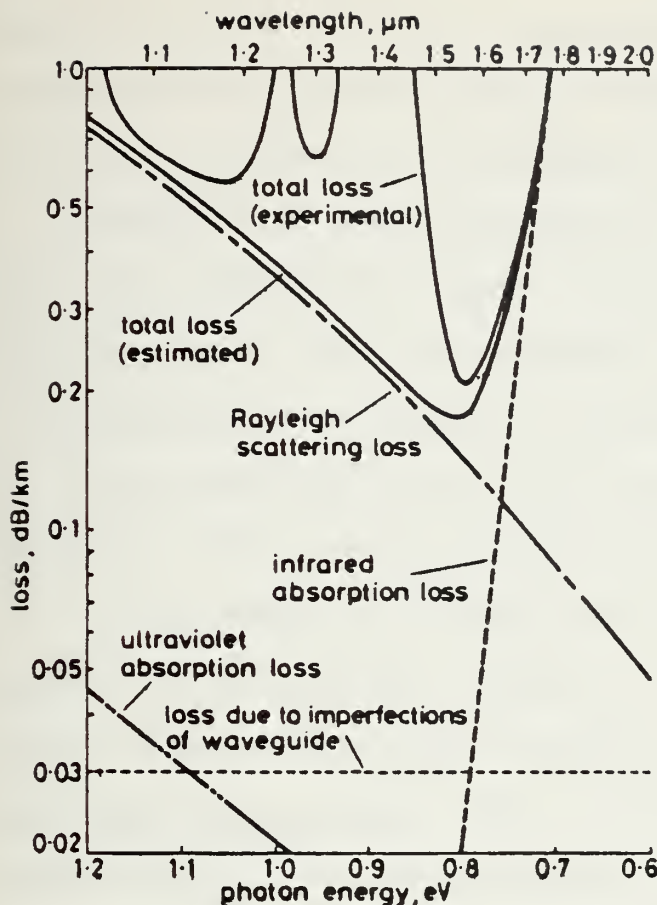


Figure 5.

Attenuation losses for silica-based (2 percent GeO_2 -doped core) fibers in the 1.0–1.8 μm region.

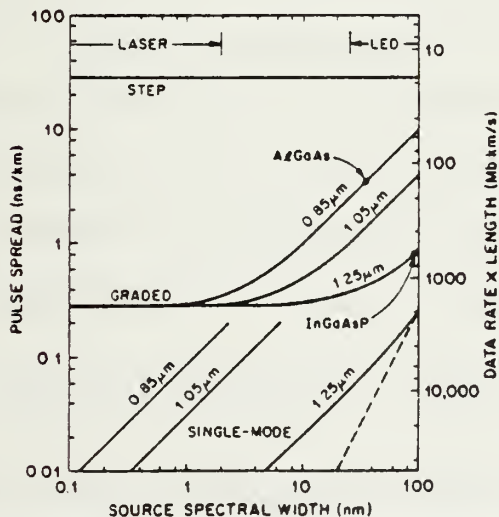


Figure 6.

Pulse spreading and transmission bandwidth (data rate-fiber length product) versus source spectral width for: multimode fiber of step-index profile, $\text{GeO}_2 \cdot \text{B}_2\text{O}_3 \cdot \text{SiO}_2$ glass, $\Delta = 0.01$; multimode graded-index fiber, $\text{GeO}_2 \cdot \text{B}_2\text{O}_3 \cdot \text{SiO}_2$ glass, $\Delta = 0.01$, bandwidth improvement factor = 100; and single-mode fiber, $\text{B}_2\text{O}_3 \cdot \text{SiO}_2$ glass, $\Delta = 0.001$. The pulse spreading and spectral width are twice their respective root-mean-square values. The dashed line corresponds to the fundamental low limit to pulse spreading in silica-based fibers

greater than 1.6 micron, the infrared absorption loss of doped silica glass becomes the dominant factor, as it sharply increases with wavelength [8].

Besides the lower attenuation, the longer wavelengths have the advantage of lower overall dispersion rates. Attenuation as well as dispersion limits the length of transmission lines between repeaters; however, dispersion or pulse spreading, also limits the data capacity of the system. There are three main causes of dispersion in fibers.

1. As frequency changes, the dimensions of the waveguide, in wavelengths, changes. This normally causes the phase term to vary with frequency, leading to so-called waveguide dispersion. This is of importance in single mode guides while for multimode guides it can be neglected since it affects only high-order modes which are attenuated to irrelevance in long lengths of fiber [8].

2. Material dispersion is due to the frequency dependence of the electrical properties of the waveguide material. It is caused by the nonlinear aspects of the refractive index with respect to transmission wavelength. Pulse spreading from material dispersion is given by:

$$\text{Material dispersion} = \left(\frac{L\lambda}{c}\right) \left(\frac{d^2 n}{d\lambda^2}\right) \Delta\lambda \quad (4)$$

where L is the length of the fiber, λ is the wavelength of transmitted light, c is the speed of light, n is the fiber

core refractive index and $\Delta\lambda$ is the spectral width of the light source. Finding a value of λ for which $d^2n/d\lambda^2$ is zero will eliminate this source of dispersion. It has been determined [8] that for pure silica a "zero material dispersion" (ZMD) point occurs at $\lambda = 1.27$ microns. Adding certain dopants can shift the ZMD point within the bounds of approximately 1.2 microns to 1.4 microns.

3. Signal distortion will occur if more than one propagating mode is excited. Multimode dispersion results from different rays of light of the same wavelength propagating through the fiber core along different paths. This results in different path lengths and therefore, different arrival times for rays launched into a fiber coincidentally. Multimode dispersion is a function of fiber length, refractive index, and type of multimode fiber -- graded index or step index. It is independent of wavelength.

Figure 6 [8] gives a clear understanding of the overall dispersion picture. When step index fiber is used, multimode dispersion is the critical cause of pulse broadening regardless of the source or wavelength. On the other hand, when graded index fiber is used along with an LED source, the longer wavelengths decrease the pulse spreading considerably.

The attractiveness of longer wavelengths is spurring the search for new materials to produce LED and laser sources in the range $1.0 \text{ micron} < \lambda < 1.6 \text{ micron}$. This year the first long-wavelength communications system was put into operation in

Sacramento, California. The system uses an LED operating at 1.3 microns. The receiver is an indium gallium arsenide p-i-n diode [9]. The best detector for the 1.1-1.7 micron range is not a clear cut choice but several high-sensitivity optical receivers that operate efficiently in this area have been developed [8]. In a proposed trans-Atlantic fiber optic cable, Bell laboratories have suggested the following:

Source: Single mode InGaAsP laser
Detector: InGaAsP p-i-n diode
Fiber: <1dB/km
Wavelength: 1.3 microns.

France will soon install an experimental fiber optic network to operate at either 1.3 or 1.55 microns [10]. This is but a sampling of the work being done in research and development of the longer wavelengths. Low-loss systems operating in the 1.1 to 1.6 micron waveband show promise of high performance with long repeater spacing due to low loss and low material dispersion of fibers in that waveband. Figures 7 and 8 graphically illustrate the fact that the greatest bandwidth-distance product or minimum dispersion wavelength coincides with one of the loss minima, 1.3 microns. Figure 8 also indicates the use of InGaAsP sources and detectors above 0.9 microns.

In anticipation of the move toward longer wavelengths, fiber manufacturers are making fibers with their lowest attenuation in the 1.1 to 1.7 micron band. Corning Glass

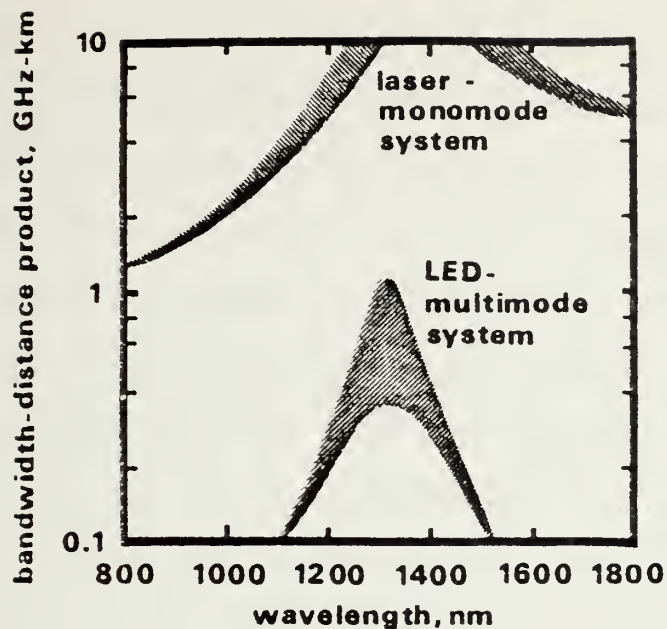


Figure 7.

THE RANGE OF BANDWIDTH LIMIT FOR LED-MULTIMODE AND LASER-MONOMODE SYSTEMS.

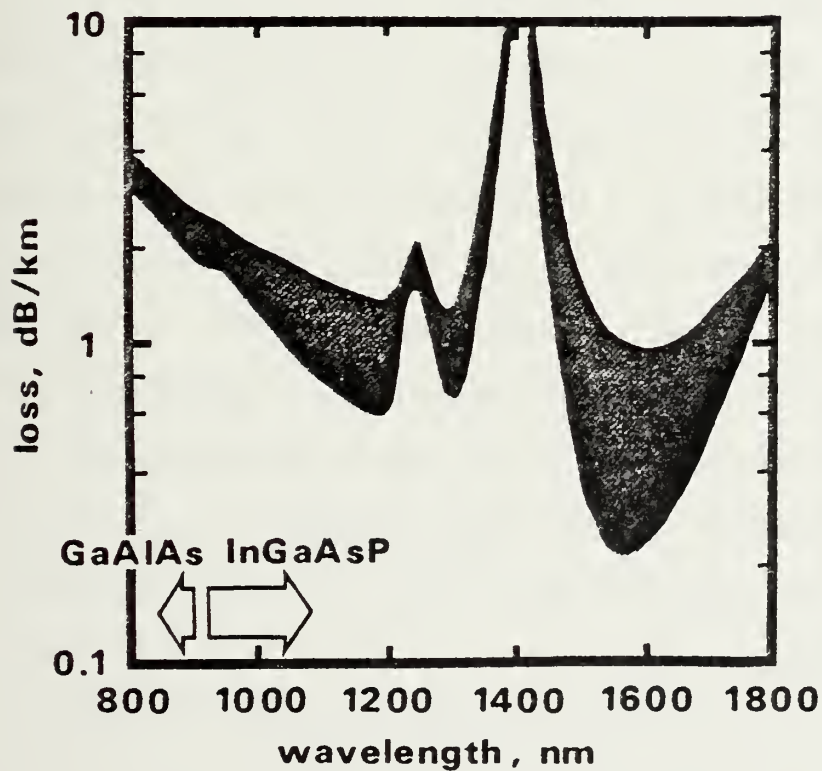


Figure 8.

THE RANGE OF LOSS SPECTRA OF FIBERS FOR LONG-WAVELENGTH OPERATIONS

Works has recently announced a line of fibers they call the Double Window Fiber (DWF). Through improvements in composition and manufacturing techniques, they offer superior performance at the wavelengths of present sources (0.8-0.9 microns) and improved attenuation performance at wavelengths proposed for second generation operation (1.1-1.5 microns). Therefore, they are both non-obsolescent and upgradeable. The attenuation is characterized for .850 microns and 1.3 microns. At .850 microns the attenuation ranges from 2.5 to 3.5 dB/km while the attenuation at 1.3 microns is about 1.5 dB lower. This difference is due to the scattering loss of the fiber discussed earlier.

If double window fibers are good, triple window fibers should be even better. With the proper choice of composition, operation optimized at 1.55 micron is also feasible [11]. Multiple window fibers are being marketed and bought for the advantage of being installed in a system today which could be later upgraded to longer wavelength operation without replacing the fiber. Another advantage to these fibers which is growing in popularity is simultaneous multiple wavelength operation. In a triple window fiber the signal capacity would be virtually tripled over a single window fiber. Germany is planning a telephone system for 1983 using fiber with low-loss windows at 0.8, 1.3 and 1.5 microns to allow for future upgrading [12]. Presently, almost all optical fiber communications systems utilize single wavelength transmissions on a fiber. By using

different wavelengths, it is possible to transmit several communications channels over the same fiber bidirectionally. This capability adds a third dimension to the conventional frequency division multiplexing and time division multiplexing which is unique to optical fibers. Actually, two-way communications over the same fiber can occur at the same wavelength if 3-dB directional couplers are used at each end [11]. Bidirectional single fiber communications and wavelength division multiplexing are receiving a lot of attention and have recently been reported on by a number of different laboratories worldwide [13-17].

One final area of fiber optic research worth mentioning is fiber optic sensors. Sensing of changes in temperature, pressure, radiation and other phenomena has been forecasted to explode into a major market in the late 1980's and the 1990's for both high and low performance optical fibers. The possible application of fiber optic sensors to the QUTR would be the development of a fiber optic hydrophone. The underwater signal from the torpedo is an acoustic wave with pressure variations. These pressure changes on a fiber mesh can modulate a highly coherent source such as a laser. The U.S. Naval Research Laboratory in Washington, D.C., is doing active research on optical fiber sensors along with several other laboratories [18, 19]. NRL has tested several sensor configurations and categorized different fiber optic sensors by frequency response, fiber type, source, and advantages.

In the next twenty years fiber optics technology will continue to develop and fulfill its tremendous potential. Attenuation will be well under 1 dB/km with low dispersion, allowing bandwidths in excess of 1 gigahertz. Attenuation will be so low that transmission will be taken for granted much as the conductivity of copper wire. High performance cable will be available at less than ten cents per fiber meter. Cost today is viewed as neither an advantage nor a disadvantage for optical fibers in general, however, the prospect for advantageous cost values in certain applications will soon be realized. By the year 2000 virtually all new installations will use fiber vice copper. Also, many copper cables will be replaced by fiber.

Undersea applications are becoming especially attractive. Broad bandwidth and low losses allow for higher data capacity and fewer repeaters. The physical size of fiber cable is significantly less than its coaxial cable counterpart. Because of the small fiber crosstalk, a number of fibers can be fabricated into a single cable. Rather than using an underwater multiplexer for the QUTR (see Figure 1) each individual hydrophone cable could be incorporated into one cable at the current multiplexer point and that cable could be run to a shore based multiplexer. By bringing the multiplexer out of the water and onto the beach, the electrical power required underwater is reduced. If signal security is a requirement, moving the multiplexer to shore produces

another advantage. The optical signal experiences almost total internal reflection. The cladding surrounding the fiber is made thick enough so that for all practical purposes, there is no field outside of the cladding. This characteristic aids in the overall security of the link.

Gone is the day when fiber optics systems needed to be proven. Today they are being improved. The majority of the improvements in second generation systems stem from the shift of operating wavelength from the near infrared, 0.8 to 0.9 microns, to the wavelength range 1.1 to 1.7 microns. Fiber optic multiplexers and sensors are two novel devices now being tested in the laboratory.

II. PROPOSED FIBER OPTIC SYSTEM

A. OVERALL DESCRIPTION AND BLOCK DIAGRAM

Figure 9 lays out in block diagram format, the test system designed to demonstrate the principles of the fiber optic system proposed for QUTR. It consists of a signal generator, digital modulator, fiber optic link, digital demodulator and signal processor. The signal generator simulates the electrical signal from the torpedo. This spaced frequency shift keyed (SFSK) signal is an analog modulated digital signal (see Figure 2). The analog modulating wave is then digitized in the digital modulator and converted into optical energy for transmission over a fiber link. A detector then converts the signal into digital voltage levels for entry into a computer for processing. Once the signal is digitized at the transmitting end, there is no need to convert back to analog at the receiving end since the signal is to be processed in a digital computer. Each section of the system will be discussed in some detail including a description of operation, output waveform, advantages, disadvantages and trade offs made in the system design.

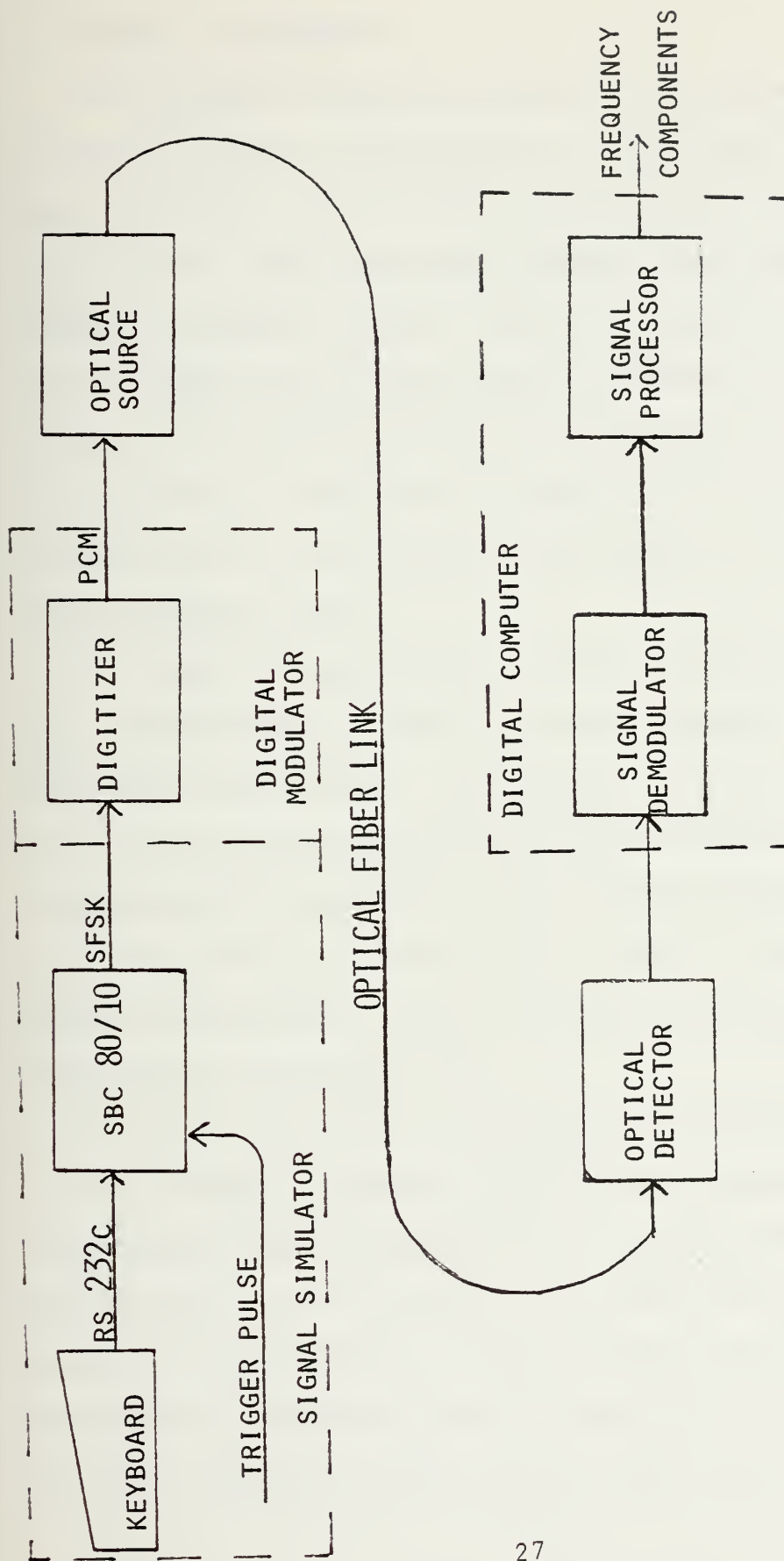


Figure 9. Proposed Fiber Optic System

B. SIGNAL SIMULATOR

The signal simulator used was a very versatile and programmably powerful minicomputer. The Single Board Computer (SBC) 80/10A is one of Intel Corporations original equipment manufacturer (OEM) computer systems. The SBC 80/10A is a complete computer system. The CPU, system clock, read/write memory, nonvolatile read-only-memory, I/O ports and drivers, serial communications interface, bus control logic and drivers all reside on a single 6.75-by-12 inch printed circuit card. The central processing unit is an Intel 8080A microprocessor chip.

In order to use the SBC 80/10A as an SFSK signal generator, an additional circuit card was required - - the PRO 80 Frequency Synthesizer. This single card unit manufactured by Proteon Associates Incorporated is mechanically and electronically compatible with the SBC 80/10A. The program for the system was written by Jay Chase of the Naval Undersea Warfare Engineering Station, Keyport, Washington, using the Intel 8080 instruction set.

The user link with this microprogrammable signal simulator is through a keyboard into an Electronics Industries Association (EIA) interface. The EIA interface used in this application was the RS-232C. This interface specifies voltage levels whereby control and data signals are exchanged between the SBC 80/10A and the keyboard of the terminal. All data signals are sent using binary serial signaling

convention. The actual hardware consists of two 25-pin plugs which can be mated together. Each pin except the ground is activated by either the keyboard or the computer; thus the pins may be regarded as directional. Each pin will, at any point in time, carry a voltage level corresponding to binary 1 or 0. These binary signal levels are used to indicate the activation or deactivation of control functions on control pins and the values of bits in the data stream on data pins. In most applications, only some of the 25 lines are actually used but they are all connected through mating of the connectors. Specifications of the RS-232C interface permit a certain degree of applications engineering leeway. There is no guarantee that any two devices with RS-232C interfaces can be connected together and be completely compatible. There are many variations of the standard interface which become strongly applications dependent [20].

The keyboard terminal used in this application was the Computer Devices Miniterm. This terminal is designed primarily to be used with a modem using telecommunication links. Communicating directly with the SBC 80/10A is different from the designed application for the terminal and therefore several wiring changes in the interface were required. Figure 10 documents the individual switch settings and wiring changes made on the Computer Devices Miniterm in order to successfully communicate. Only those lines required in the RS-232C interface were connected.

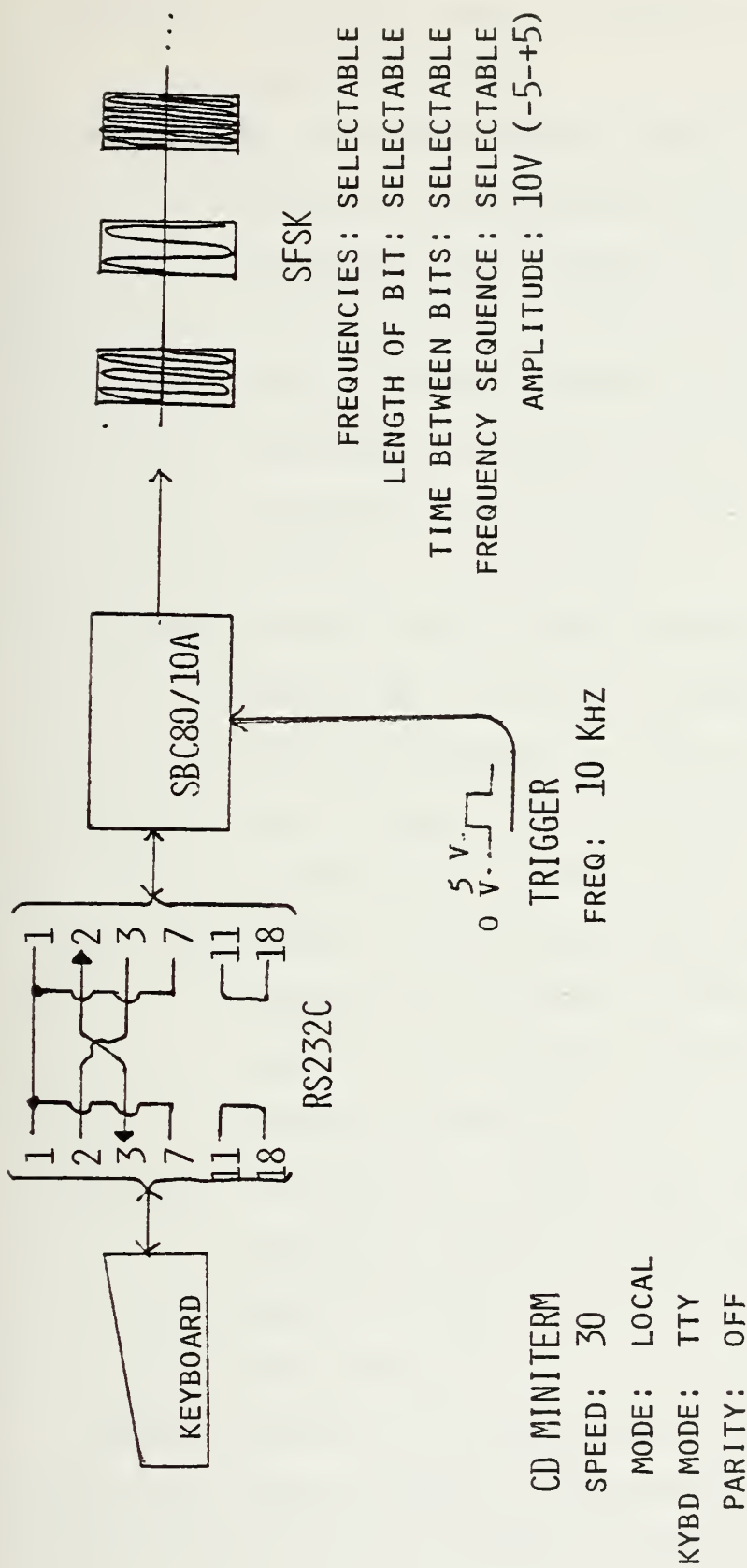


Figure 10. Signal Simulator Setup

- Pin #1: Protective Ground-electrically bonded to the equipment ground.
- Pin #7: Signal Ground/Common Return - establishes common ground reference potential for all other interface lines except line #1. Strapped to Pin #1 on computer and terminal interface.
- Pin #2: Transmit Data - Serial data on this circuit is generated by the receiver with logic "1" voltage level between -3 V and -12 V and logic "0" between +3 V and +12 V.
- Pin #3: Receive Data - Serial data on this circuit is generated by the data terminal. Logic "1" level is between -3 V and -12 V into a 3K Ω load. Logic "0" level is between +3 V and +12 V into a 3K Ω load.
- Pin #11: Local - a TTL output from the terminal indicating the placement of the terminal mode switch into the LOCAL mode when the voltage level is less than +0.8 V.
- Pin #18: Local Full - a TTL signal input which will place the terminal in full duplex mode when jumpered to pin 11 (used for hardwire connection only).

Program control is accomplished through the keyboard using a few simple commands. Switching power to the SBC 80/10A initializes the program. From there, any one of

eight preprogrammed SFSK signals, called "setups" in the program, may be selected. The capability also exists to generate a custom signal from the keyboard by specifying modulating frequencies, bit time, space time, and frequency sequence. Referring to Figure 2, the setup required to simulate the Band 1 telemetry signal would consist of the following.

FREQUENCY A (HZ) = 0033325

FREQUENCY B (HZ) = 0034755

FREQUENCY C (HZ) = 0036245

FREQUENCY D (HZ) = 0037800

TIME OF BITS (μ S) = 001500

LENGTH OF SPACE (μ S) = 011000

SEQUENCE = A_B_C_D_

These specifications would produce a SFSK signal consisting of a 1.5 msec. burst of 33.325 kHz., followed by an 11 msec. space, a 1.5 msec. burst of 34.755 kHz., an 11 msec. space, a 1.5 msec. burst of 36.245 kHz., an 11 msec. space, and a 1.5 msec. burst of 37,800 kHz.. This sequence will repeat on the next positive going pulse from the trigger (see Figure 10). The programmed sequence may have up to 126 frequencies and spaces in place of the eight (four frequencies and four spaces) shown above.

The signal simulator is a very handy and convenient device to simulate the signal transmitted from the torpedo being tracked. It is very versatile in that almost all

components of the signal may be altered for experimentation. When used alone, however, there are two deficiencies that must be noted. Both deficiencies stem from the fact that the signal out of the SBC 80/10A simulates the clean signal transmitted from the torpedo and not the noisy signal received at the hydrophone.

First, there is no provision for adding in the severe multipath problem mentioned earlier and illustrated in Figure 2. One possible method of introducing multipath interference to the signal would be to run the output of the SBC 80/10A through an analog delay device. Single chip "Bucket Brigade" devices such as the SAD1024A may do the job with a minimum of external circuitry. The SAD1024A has two separate 512-stage shift registers which can be used independently or in combination to provide a continuously variable electronic delay to create reverberation, echo or phase shift.

The second deficiency of the system is that no provision is made for the occurrence of a Doppler shift in frequency. The Pro 80 Frequency Synthesizer has the capability of rapid frequency slewing with extremely fine granularity. The maximum frequency update rate is limited by the microprocessor speed. The SBC 80/10A microcomputer has a 480 nanosecond clock period and this corresponds to a minimum time required to increment the output frequency of 24 microseconds per

increment. This means that during one pulse of 1.5 milliseconds, as many as 62 frequency increments could occur.

C. SIGNAL MODULATION

The modulation scheme selected is important to the total system architecture of any communication system. The information to be transmitted may be encoded in any of several ways; the proper choice depending on the characteristics of the system. Modulation techniques can be grouped into one of two categories - - analog or digital. After a brief discussion of analog modulation, several different digital schemes will be investigated and compared. The basic difference between modulation of optical carriers and of rf carriers stems from the nature of the devices used. In optical systems the intensity (square of the electric field) is modulated directly rather than the amplitude as in rf systems [21].

Analog modulation can be further divided into two categories: continuous analog modulation and sampled analog modulation. In continuous analog modulation the source is not encoded but rather the information signal varies continuously with amplitude (AM), frequency (FM), phase (PM) or intensity (IM). IM analog transmission is the most compatible with existing light sources. The value of the intensity is directly proportional to the value of the signal and therefore IM analog modulation requires great device

linearity. In general, a laser source will produce more linear operation than a light emitting diode source.

Sampled analog modulation, also referred to as pulse modulation, requires periodic samples of the information signal which are encoded through one of several parameters of the intermittent carrier. In other words, a pulse has a varying amplitude, duration, or time of occurrence according to the information sample. Sampled analog modulation has been confused with digital modulation because of the individual pulses and sampling involved. If the pulse has continuously varying values of amplitude, duration or time occurrence the scheme is analog. If there is a finite number of discrete values of amplitude, duration, etc., then the scheme is a digital one. Analog systems require less bandwidth than digital systems; however, bandwidth is not usually a constraint in optical fiber systems. Digital systems require greater processing speed than analog systems, but this also is not a problem with modern semiconductor technology. The properties of optical systems make them well suited to reap the benefits of a digital modulation scheme.

The advantages of using a digital modulation scheme include the following:

1. Digital signal regeneration may be accomplished at the repeater or receiver with a minimal amount of noise as compared to analog signal regeneration. In an analog

system, noise, once introduced, cannot be eliminated and the signal is degraded accordingly. This is not the case in digital transmission. As long as the receiver can make a binary decision on the presence or absence of a pulse, the perturbations of the signal due to the preceding transmission section are eliminated.

2. Substantial bandwidth is available in optical systems and digital modulation can utilize that bandwidth to good advantage.

3. If multiplexing is required, the frequency division multiplexing used for analog systems is more expensive than the time division multiplexing used for digital systems [6].

4. The use of a digital computer at the receiver site for processing of the signals means that the signal must be digitized at some point prior to entry into the computer.

Six different digital modulation schemes will be discussed: Pulse Intensity Modulation (PIM), Pulse Width Modulation (PWM), Pulse Position Modulation, Pulse Frequency Modulation (PFM), Delta Modulation (DM), and Pulse Code Modulation (PCM).

Pulse Intensity Modulation is not particularly attractive. Discrete intensity levels are set and the source intensity becomes one of these levels according to the message input. As in the analog case, this requires a highly linear source and exact attenuation measurements from transmitter to receiver in order to correctly decode the signal.

A pulse width modulated waveform consists of a sequence of pulses, the width of each pulse being proportional to the values of a message signal at the sampling instants. The problem here is with dispersion. The transmitted pulse width will always be less than the received pulse width. This will increase the difficulty of the receiver to correctly decode the signal.

Pulse Position Modulation consists of pulses in which the displacement from a specified time reference is proportional to the sample values of the information bearing signal. PPM is particularly attractive for optical communications systems because the optical source can be operated at a low duty cycle to extend the lifetime of the device. PPM systems share with PWM systems the problem of dispersion mentioned. Generally, PPM will be useful at low bit rates where pulse broadening is negligible.

Pulse Frequency Modulation is a method of pulse modulation in which the information signal is used to frequency modulate a carrier wave consisting of a repetitive pulse train. The PFM approach is being tested by the British Post Office in Milton Keynes, a town north of London. Even though the signal consists of a train of pulses, they consider it an analog system because the electrical modulators and demodulators work on analog principles. PFM can be considered frequency modulation of a square wave. The pulselike nature of the PFM signal lowers the susceptibility to source and

detector nonlinearities which are critical in conventional analog systems as mentioned earlier. The other disadvantage of analog systems however, still holds. Noise picked up during transmissions is passed on and amplified by repeaters [12].

Delta Modulation was invented in 1946 as a method of analog-to-digital conversion using principles not in common usage at the time. DM pulses represent binary decisions based on whether the difference between the modulating signal and the approximation of the signal at the time of sampling is positive or negative. The encoder contains a difference circuit which subtracts the output of a pulse integrator from the modulating a signal. The difference between the actual signal and the approximated value then controls the pulse generator to produce either positive or negative pulses of uniform duration and of constant amplitude for that pulse interval. A comparison made by ITT Federal Laboratories between a delta modulation and a pulse code modulator (to be discussed next) shows that above 40 kilobits per second, PCM was superior in signal to noise ratio [22]. One advantage of DM, however, is that synchronization is not required at the receiver to demodulate the signal. The decoder consists of an integrator identical to the one in the encoder and a low pass filter.

Pulse Code Modulation will be shown to be well-suited to transmission over optical fiber systems. PCM means that an analog modulating wave is sampled, quantized, and coded. Standard values of a quantized wave are indicated in the modulated wave by a series of coded pulses that, when decoded, indicate the standard value of the original quantized wave so that it may be reconstructed. When using optical sources, the codes will usually be binary, where the code for each quantized level will consist of pulses and spaces. Besides having all the advantages of digital transmission, PCM possesses two additional advantages. A single pulse only carries a fraction of a bit of information similar to spread spectrum techniques mentioned in an earlier work on QUTR [3]. The analog value of a wave is set to the closest quantized level and then that level causes an n-bit pulse train to be transmitted.

PCM is computer compatible. The string of coded pulses representing an analog value can even be the American Standard Code For Information Interchange (ASCII) or Binary Coded Decimal (BCD). What this means is that very little if any code conversion is required prior to the signal being input to the computer.

One interesting characteristic of PCM important to the QUTR application is the fact that the frequency of the analog signal can be recovered directly from the digital pulse stream. There is no need for a digital to analog converter

at the receiving site. All the information in the SFSK signal is contained in the frequency of the modulating wave. Therefore, PCM seems to be ideally suited as the digital modulation technique for the QUTR because of the following advantages:

- binary detection has the greatest noise immunity
- a single pulse carries only a fraction of a bit of information
- excellent compatability with a computer processor
- the frequency of the analog wave may be recovered without demodulating the PCM signal

PCM encoding entails three steps as indicated in Figure 11: sampling, quantization and binary word assignment. Sampling theory states that to be recovered completely, a signal must be sampled more than twice per cycle. Another way to describe the limitation is by the Nyquist frequency, which is equal to one-half the digitizing rate. No signal at or above the Nyquist frequency can be recovered. If a signal is sampled less than two times per cycle a phenomena called aliasing can occur, in which the reconstructed signal turns out to be a lower-frequency version, or alias, of the actual signal. Aliasing can only be prevented one way - by sampling a signal more than two times per cycle of the highest frequency it contains. The highest frequency planned for QUTR is 49.407 kHz. Sampling rate must be greater than 98.814 kHz or essentially 100 kHz.

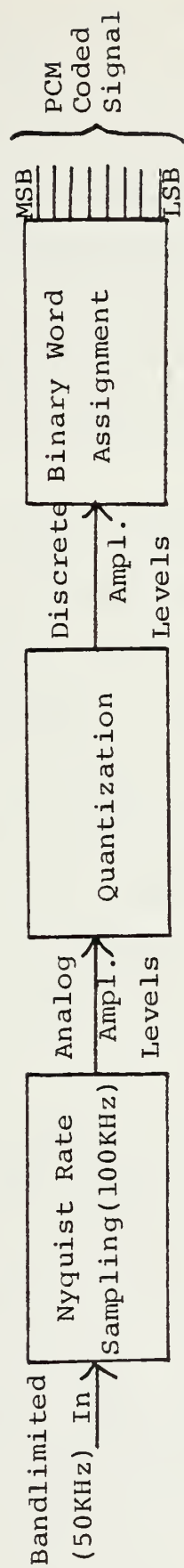


Figure 11. PCM Encoding

Quantization is the process of assigning a set of discrete output levels to analog amplitude levels. It is here where the primary error is introduced for this application. Quantizing error is the difference between the value of the analog input and the digital output.

Finally, the quantized value is coded into n-bits from most significant bit (MSB) to least significant bit (LSB). It is this code which may be ASCII, BCD or straight binary.

The block diagram (Figure 12) of the PCM transmitter designed and built shows the analog wave input to an analog to digital converter (ADC). The ADC used was Datel Systems Inc., Model ADC-EH8B1. Of the several possible methods of analog to digital conversion, the most common method and the one employed in this converter is successive approximation. The successive approximation converter is known for its high resolution combined with high speed. It operates at a fixed conversion time; independent of the value of the analog input.

Referring to Figure 12, the 2 MHz system clock is fed through a divide-by-twenty counter, giving a 100 kHz sample rate for the ADC. This is above the Nyquist sampling rate of 98.814 kHz mentioned earlier. The actual conversion time of the ADC-EH9B1 is 4 μ sec. When the conversion is complete, the end of convert (EOC) status line goes low indicating that the parallel data out is valid. It remains low until

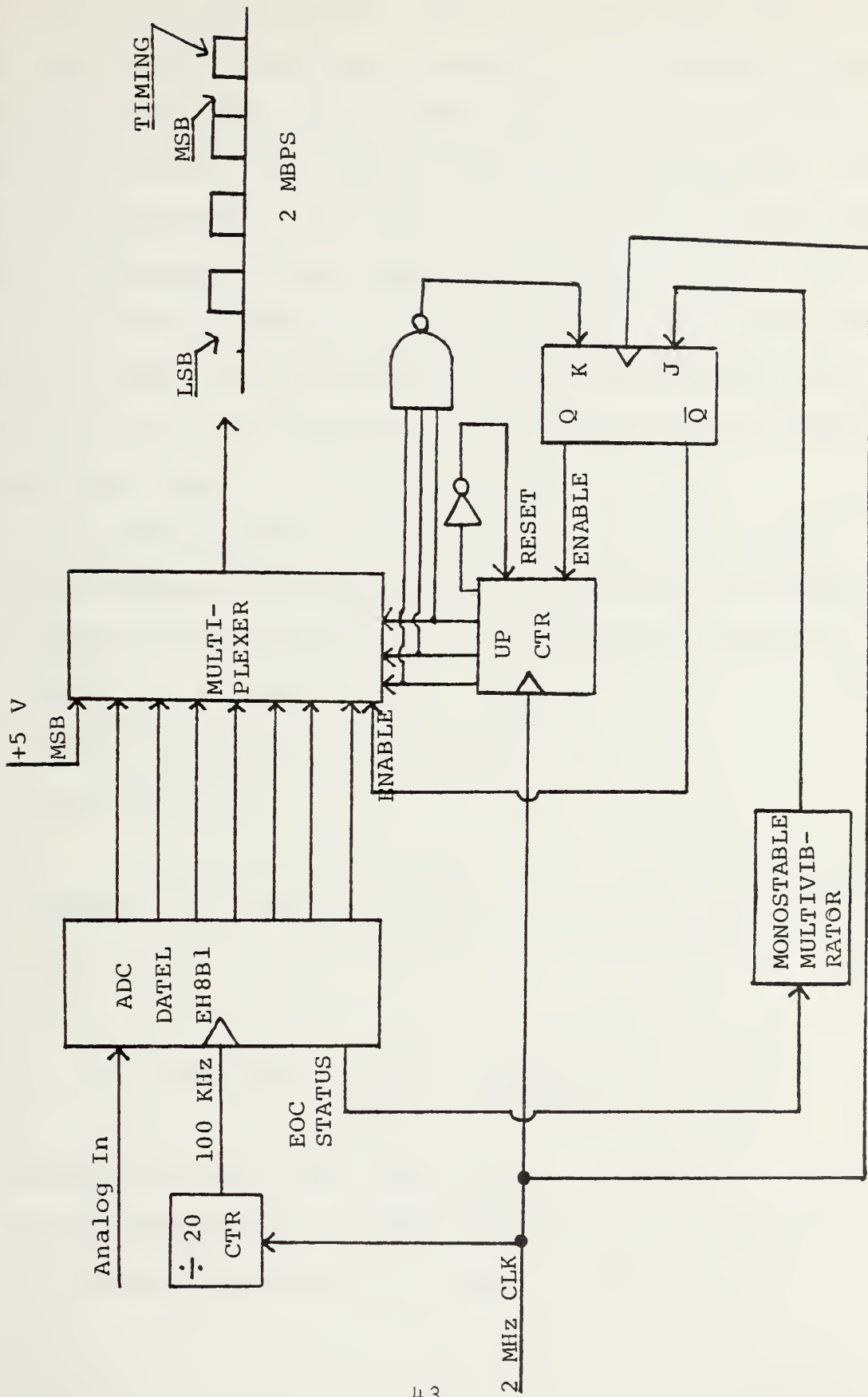


Figure 12. Block Diagram of System Transmitter

the next clock pulse, which causes it to go high again. The EOC status line transition from high to low triggers a pulse from the monostable multivibrator which enables an up counter and multiplexer. The counter counts from 0000 to 0111. On the very next clock pulse the counter is reset to 0000 and turned off until the next sample has been converted. The result of this section of the circuit is to sample the eight parallel inputs and serialize them for transmission. The first bit is used for timing in the receiver and is always transmitted high.

Using seven outputs of the ADC result in $2^7 - 1$ or 127 possible discrete sampling levels. By referring to Figure 13, the actual transmission rate can be figured as follows:

$$\text{Timing bit duration} = T_1$$

$$\text{Seven information bits duration} = T_2$$

$$\text{Lapse time} = T_3$$

$$\text{Telemetry bit Rate} = \frac{1}{T_1 + T_2 + T_3} = \frac{1}{(.5 + 3.5 + 6) \times 10^{-6}} = 100 \text{ KBPS} \quad (5)$$

$$\text{Baud Rate} = \frac{1}{T_2 / 7} = \frac{1}{3.5 \times 10^{-6} / 7} = 2 \text{ Mbaud} \quad (6)$$

Confusion can arise here since one bit of telemetry information is represented by seven PCM bits, one timing bit and a dead time of approximately 6 μsec . A PCM bit period is

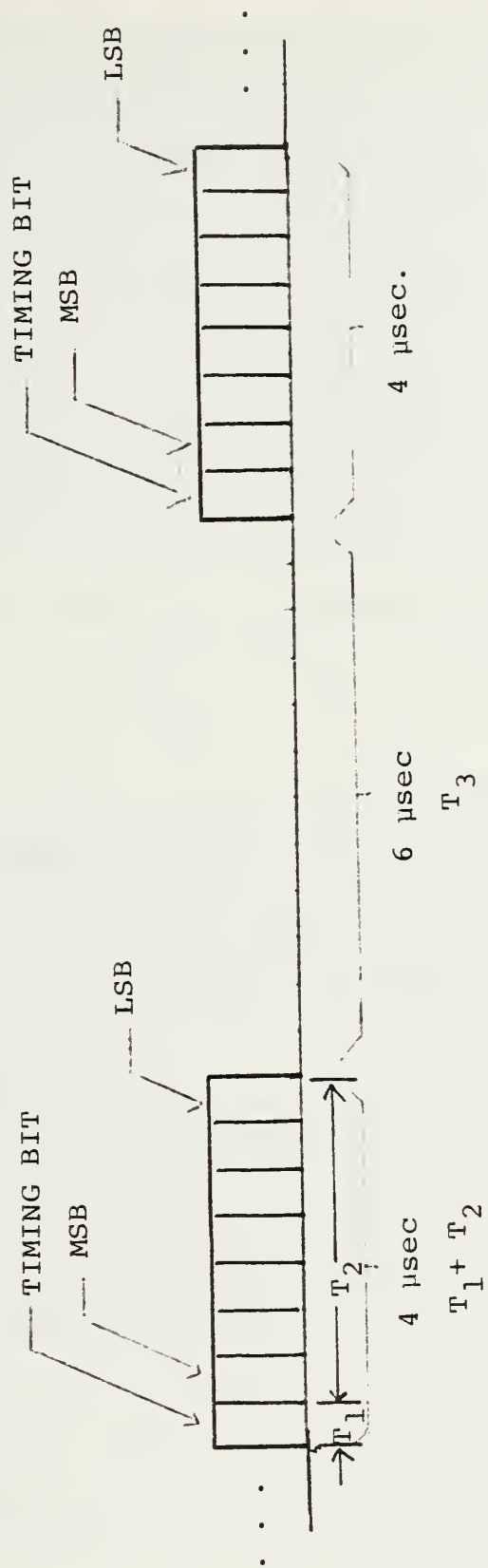


Figure 13. Signal Timing

approximately .5 μ sec. Therefore, one bit of telemetry information is sent every 10 μ sec giving an information transmission rate of 100 KBPS as shown in Figure 13.

Figures 14-19, taken from the multiplexer output, show the PCM signal just prior to conversion into optical power. In Figure 14, only the timing bit is seen (all other bits are zero) indicating that the modulating wave is at -5 volts. All bits in the PCM word in Figure 15 are high except the MSB, indicating the wave value at this point is -0.04 volts. This is just prior to the zero crossing. The next digital step (Figure 16) indicates the analog wave is now crossing zero. Finally in Figure 17, the wave is at its maximum value of +5 volts. Figures 18 and 19 are randomly chosen samples. It is easy to see that the analog wave is at some voltage greater than zero in Figure 18 and at some voltage less than zero in Figure 19. This observation can be made simply by looking at the MSB.

D. OPTICAL TRANSMITTER

The optical transmitter converts an electrical signal into an optical signal by modulating the output of a light source, usually by varying the source drive current.

Solid state light emitting diodes (LEDs) and laser diodes are the two main sources for optical fiber transmission since their output can be rapidly controlled by varying their bias current. Additional attractive features

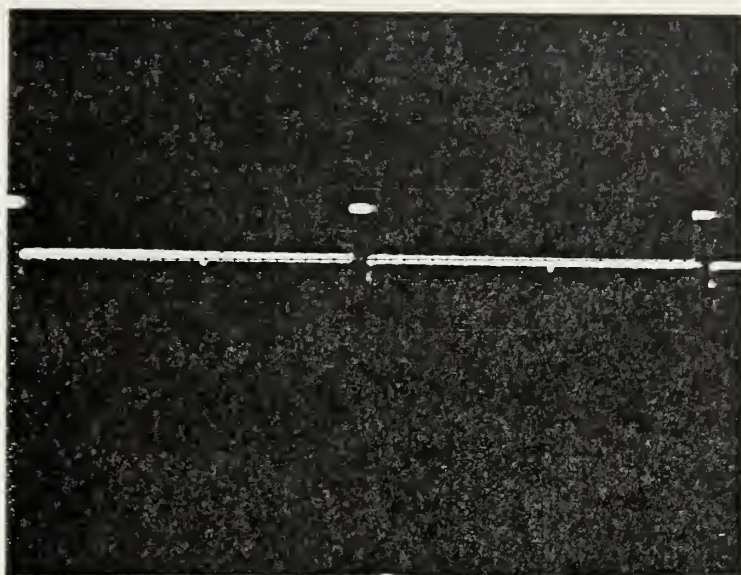


Figure 14. Example of PCM Signal with Only Timing Bit Present

Analog Wave Value: -5 V.
 2 μ sec/DIV
 5 volts/DIV

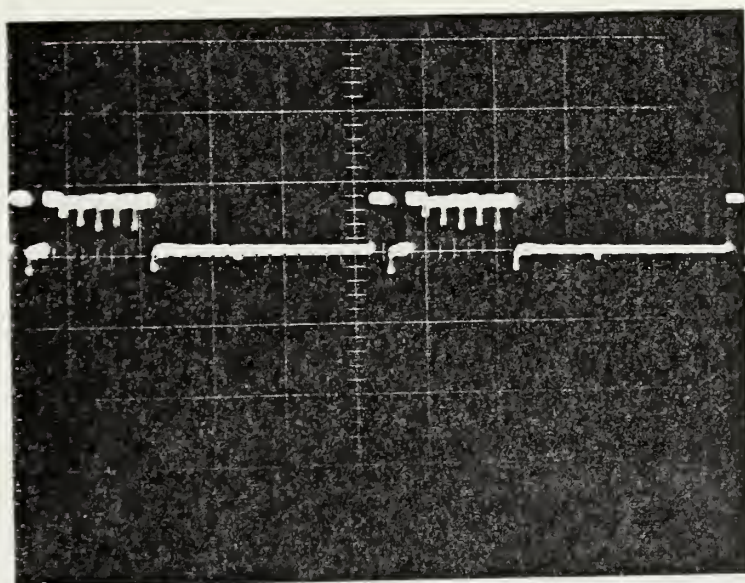


Figure 15. Example of PCM Signal

Analog Wave Value: -0.04 V.
 2 μ sec/DIV
 5 volts/DIV

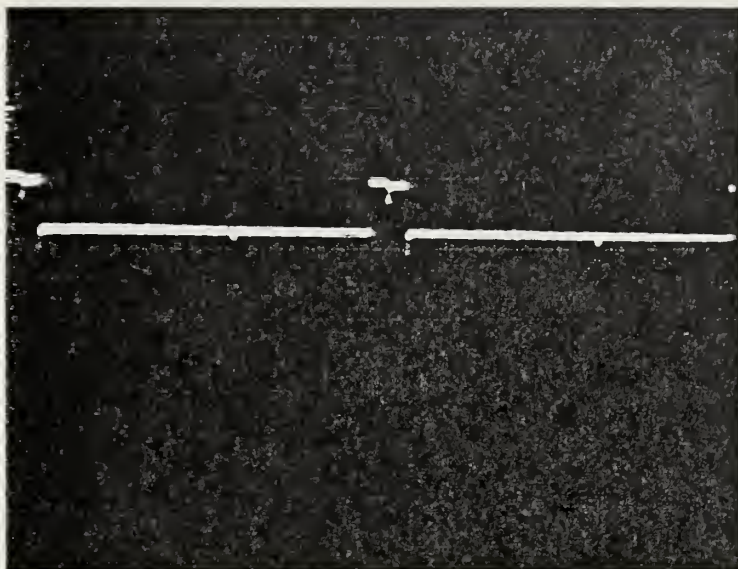


Figure 16. Example of PCM Signal
Analog Wave Value: 0 V
2 μ sec/DIV
5 volts/DIV

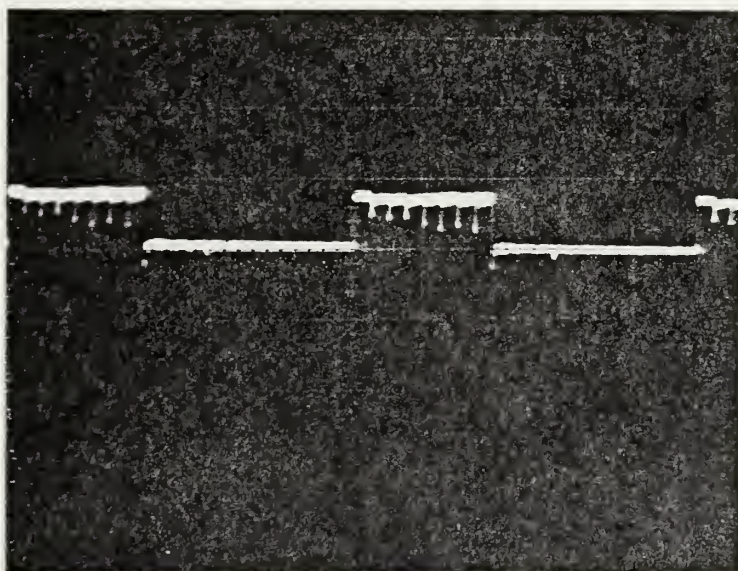


Figure 17. Example of PCM Signal
Analog Wave Value: +4.96 V
2 μ sec/DIV
5 volts/DIV

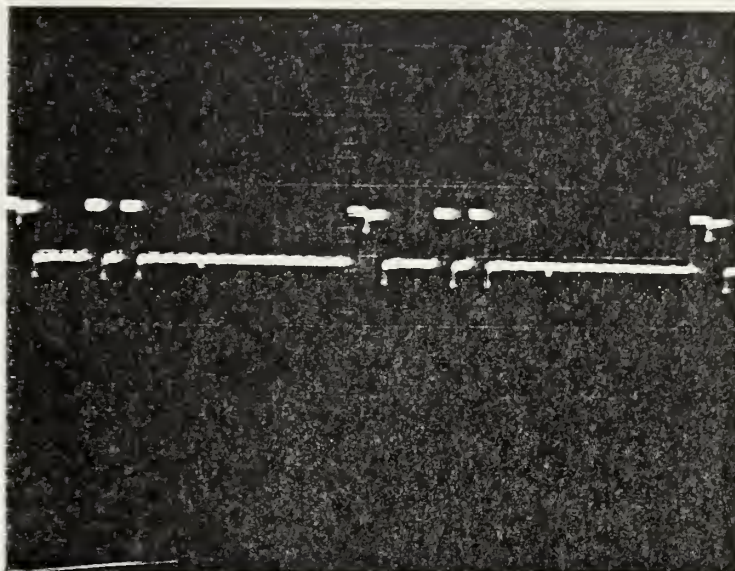


Figure 18. Example of PCM Signal
Analog Wave Value: +0.20 V
2 μ sec/DIV
5 volts/DIV

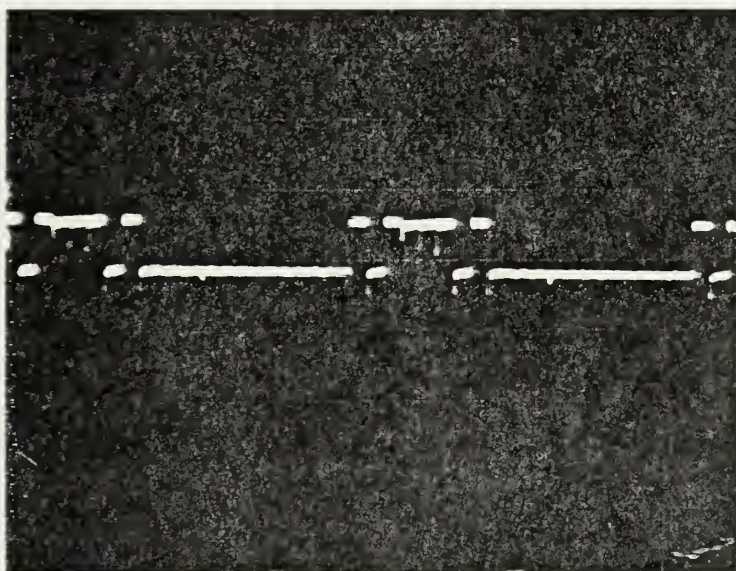


Figure 19. Example of PCM Signal
Analog Wave Value: -0.12 V
2 μ sec/DIV
5 volts/DIV

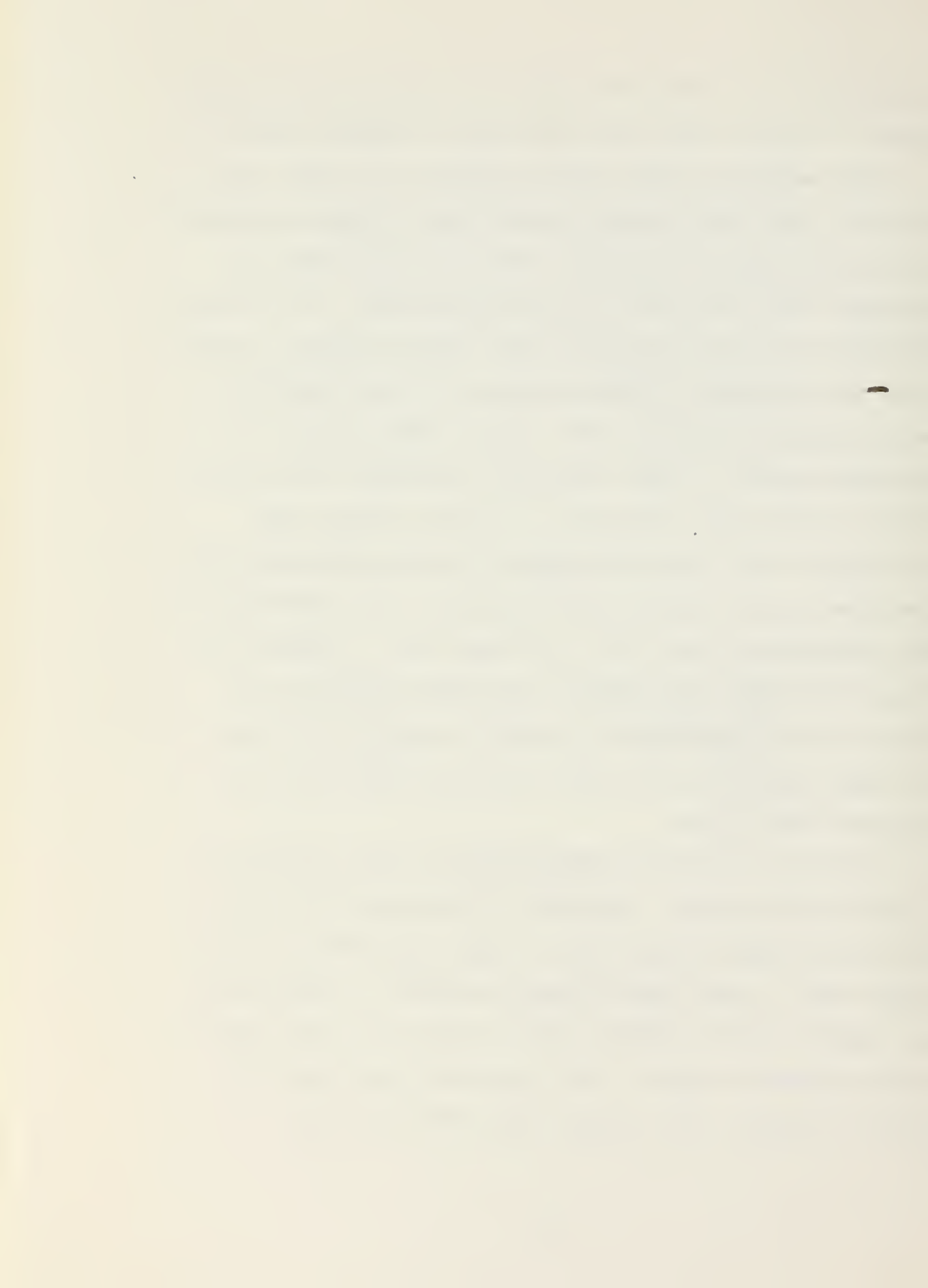
include: high brightness, small size, emission wavelength and low drive voltage. There are some definite advantages to be realized by using a laser source, mainly because of its coherence and all the implications thereof: large bandwidth, high power densities, small divergence angle, monochromaticity, linear polarization [23]. Lasers can generally produce 10 dB or more optical power than LEDs can produce. Coupling losses from the source to the fiber are also lower for lasers due to their greater power output and smaller divergence angle. Typically, 10 dB more power can be coupled into a fiber from a laser than from a LED.

As with every real-world device, there are certain trade-offs with a laser source that must be considered. One important requirement for an optical source is that it be capable of stable, continuous operation at room temperature for years. The laser must be operated in a restricted current range just above its lasing threshold current. This threshold current may change with time and temperature thereby requiring laser drive circuits to employ special feedback or electronic drive circuits. The cost of laser sources is generally two to four times that of LED. For a single point to point communications system that initial cost is not as important as it is in a system such as the QUTR where there would be a number of sources; one at each hydrophone. The threshold current for lasers is about double the current requirement of LEDs. This is another important

consideration for the QUTR where each hydrophone must have a source of power, either from the beach or internal supply.

Light emitting diodes are the simplest of solid state sources. They have adequate output power, optical bandwidth, and can be directly modulated. Their low cost and long life make them the choice for this application. The primary limitation is their relatively wide output spectrum. Therefore the bandwidth is limited primarily by the fiber dispersion characteristics rather than by fiber losses. As mentioned earlier, longer wavelength operation could drastically reduce this limitation. In fact, InGaAsP LEDs operating at the longer wavelength have been fabricated for some time and now actually perform better than the GaAlAs LEDs operating in the 0.8-0.9 μm range [24]. Because the electrical signal can directly drive the LED source and because of the simplicity of control circuitry, low cost and high reliability, the LED source was chosen for the proposed QUTR system.

The LED is primarily characterized by its radiance at a given drive current. Radiance is the radiant flux per unit solid angle per unit area. Some LED sources are purchased with a short fiber pigtail attached. In that case the radiant flux or optical power coupled into the fiber is usually given in watts. Other important parameters are listed in Table 1 for a Laser Diode IRE-160FB LED.



LIGHT EMITTING DIODE
IRE - 160FB

	<u>Min</u>	<u>Typ</u>	<u>Max</u>
Total Optical Power Out:	40 μ w	50 μ w	
(into pigtail with 100 ma DC current)			
Forward current DC:		100 ma	150 ma
Voltage: Forward at 100 ma DC:		2 V	
Reverse:			3 V
Peak wavelength of emission:	.805 μ m	.820 μ m	.835 μ m
Spectral Width (3 dB points):		.040 μ m	
3 dB Optical Power Bandwidth:		40 MHz	
Rise Time:		14 ns	

Table 1. Laser Diode Laboratories Inc.
IRE 160FB LED Specifications

The LED drive circuit (Figure 20) designed for the QUTR is similar to one used by the Naval Ocean Systems Center (NOSC) in San Diego, California. The primary advantage of this circuit is the fact that it is TTL compatible. The digital signal from the PCM circuit is fed directly into one of the inverters which presents one TTL load. The inverted signal is then fed to five inverters in parallel. Since each inverter will actually sink about 20 ma, the LED drive current of 100 ma is achieved. In order to determine the prebias point of the LED, a plot of the I-V characteristic of the diode was made (Figure 21). Prebiasing is one method of increasing the speed of response of the LED and therefore the bandwidth. When the LED is off, a small trickle current (less than 5 ma) flows so that the LED is not completely off. When the LED is turned on by the paralleled inverters sinking current, the 40 Ω resistor acts as current limit so as not to overdrive the LED. In order to further increase the speed of response the dashed portion of the circuit may be added. At turn-on, the capacitor looks like a short circuit thereby decreasing turn-on time. Once the LED is on, the capacitor acts as an open circuit permitting current to flow only through the 40 Ω resistor.

Although Table 1 indicates the typical optical power output is 50 μ watts, the actual power output was experimentally measured in the circuit as 72 μ watts or -11.35 dBm. This value will be used later in some power budget calculations.

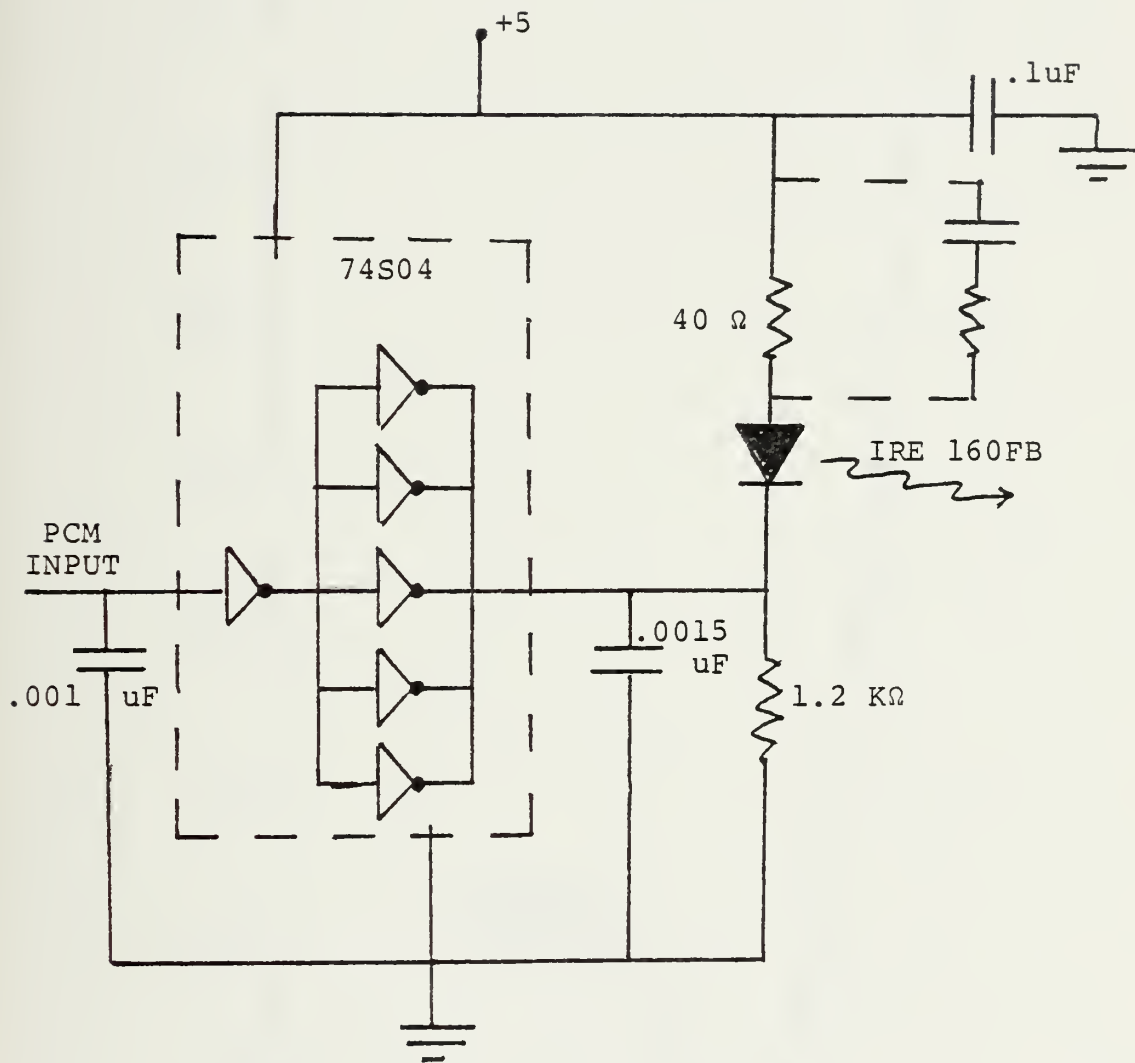


Figure 20. LED Transmitter Circuit

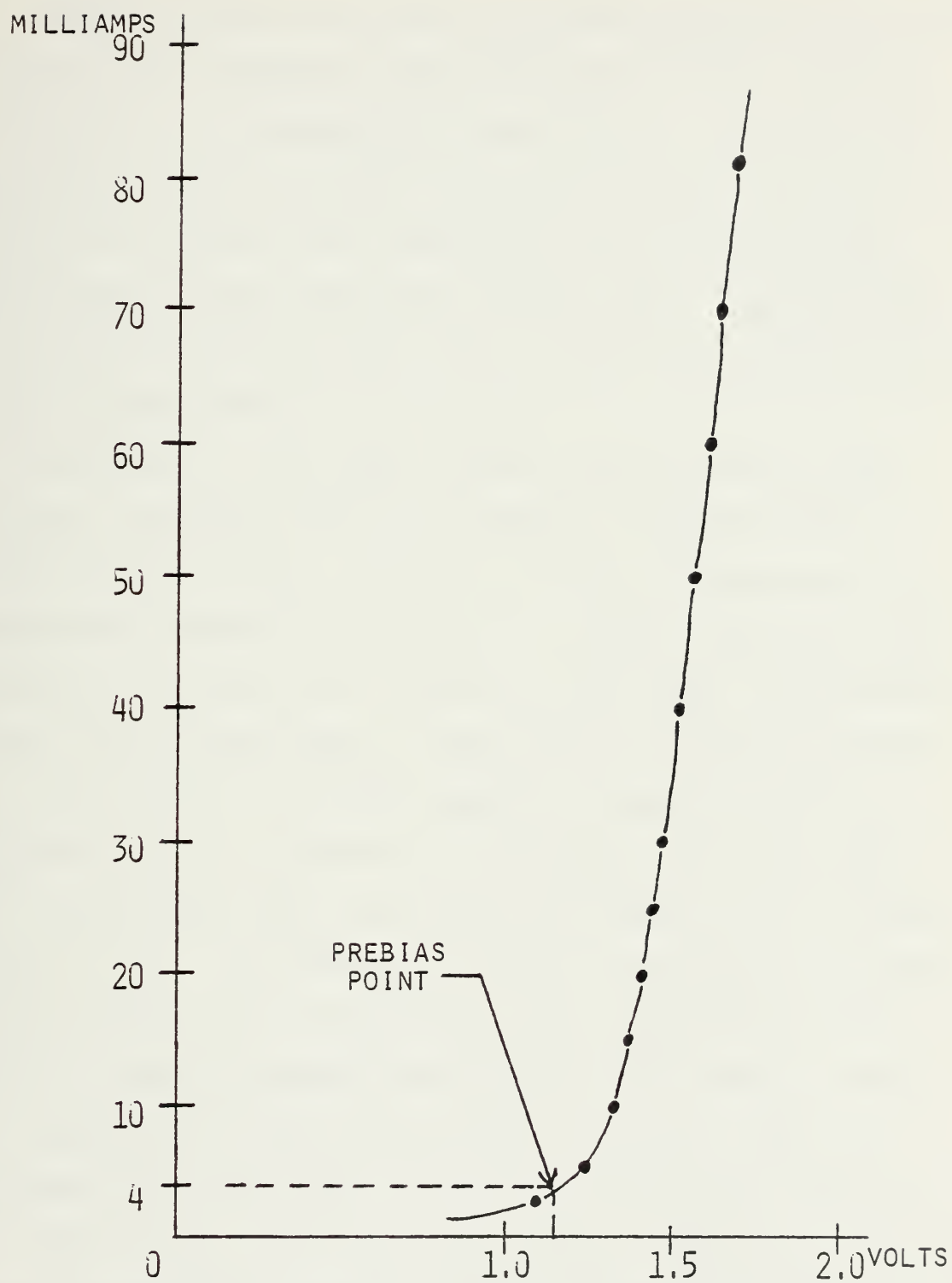


Figure 21. IRE 160FB LED V-I Characteristic

E. FIBER LINK

Optical fibers are similar to coaxial cable only in that they are most accurately described as an optical waveguide with a number of propagating modal states. One major difference is that the optical radiation becomes the signal carrier and as such its frequencies are far above those encountered in the electronic signal region. Consequently, the method of signal transmission consists of modulating the optical power output of the source.

Selection of the proper optical fiber is one of the critical considerations in the design of optical fiber communication systems. Since the fiber's attenuation is wavelength dependent (see Figure 4) and the dispersion properties of a fiber are a function of the fiber construction, fiber choice establishes an upper limit on system bandwidth and transmitter-to-receiver spacing. Engineering considerations in the selection of the proper fiber and cable for the QUTR have been researched and reported on in earlier works [2, 3]. The primary new trends that need to be emphasized are the lower attenuation values combined with the shift to longer operating wavelengths. The primary cause of attenuation at lower wavelengths in silica fibers is Rayleigh scattering which decreases as the fourth power of the wavelengths. At longer wavelengths, Rayleigh scattering becomes negligible, however, infrared absorption begins to dominate as shown in Figure 5. Doping of the fiber with

certain elements will affect the exact optimal wavelength of operation. This wavelength should coincide with the source wavelength and highest spectral response of the detector.

For the QUTR, the relatively slow bit rate of 2 MBPS, means that dispersion or pulse broadening is not the critical problem. A good quality fiber such as ITT's T-200 series with a dispersion of 3.5 ns/km is adequate to transmit the PCM signal from hydrophone to the beach. Fiber attenuation will, however, prove to be a critical factor in fiber selection. A sample power calculation and bandwidth calculation will be made in Section H of this work.

Besides the actual fiber cable, a fiber link also consists of connectors. Connector installation was the largest single nightmare encountered in the experimental work associated with this paper. Although the connectors used in the laboratory system would not be the same used in an underwater environment the problems encountered will be similar. In addition, the QUTR will have the problem of the water tight integrity of the connector. The most frustrating problem is lack of connector standardization. At present a variety of approaches to the connector problem have led to customized and unique designs on an individual system basis.

Fiber optics connectors are not the simple devices that are common in the electrical connector field. Many fiber

optic connectors tend to have more bulk than their electrical counterparts and their use involves various splicing and epoxy casting and polishing steps not required in the electrical domain. The various connector designs by manufacturers are radically different and incompatible. Most designs rely on some type of precise fiber-to-fiber alignment in the connector mechanism to provide a loss of 0.5 to 3.0 dB. These connectors range in price from about 3 dollars to over 60 dollars per connector.

Two different connectors were applied to single fiber optical cable. Both connectors required the use of epoxy for securing the fiber in the connector. A successful termination was made using an Amphenol 906-110-5001 connector. This connector employs the use of four touching cylinders placed in a hollow cylinder as shown in Figure 22. The fiber is then guided down the center of the hollow cylinder in such a way that the four cylinders act as alignment guides. Epoxy is then drawn into the hollow cylinder to secure the fiber. Finally, the four cylinders and fiber extend slightly from the end of the connector so that they may be ground and polished down to the required smooth surface.

A number of terminations were attempted using a Cannon ITT FOT-FJ series single fiber connector shown in Figure 23. Although the ITT manual for terminating these type connectors was followed as closely as possible, none of the terminations made were successful. The connector design permits termination

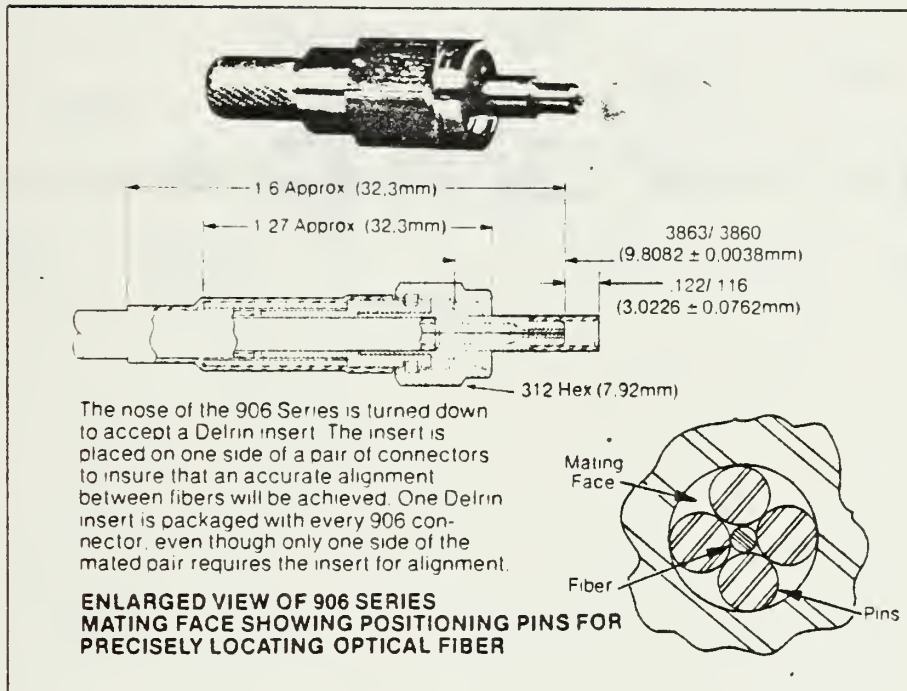


Figure 22. Amphenol 906 Series Fiber Optic Connector

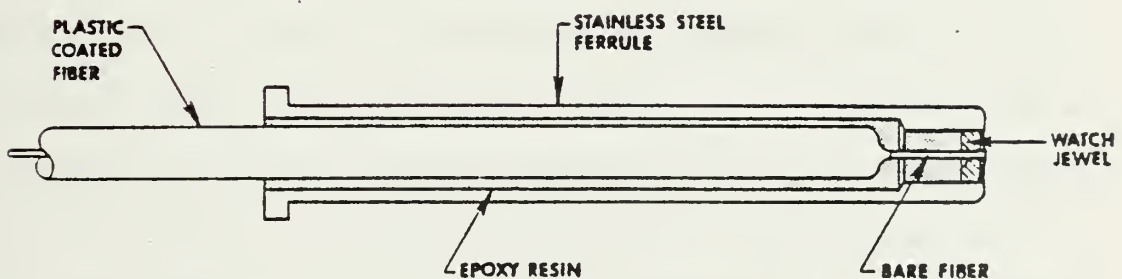
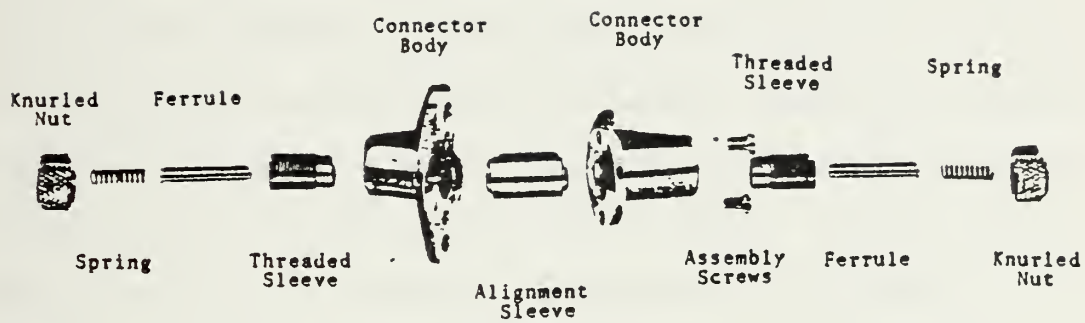


Figure 23. Cannon ITT FOT-FJ Series Fiber Optic Connector

of fibers with diameters ranging from 50 μm to 250 μm . This flexibility is achieved through the use of a jeweled ferule illustrated in Figure 23. The sapphire jewel used is a standard watch jewel. One side of the jewel is cup shaped and serves to guide the fiber into the appropriate size hole. The outside diameter of the fiber used (T-203) was 125 μm and therefore a jeweled ferule slightly larger was used as stated in the ITT manual. Epoxy was then drawn into the ferule using a syringe and rubber tubing. Finally, the jeweled end of the assembly is ground and polished.

To test the connector, an optical power meter was used. First, in order to test for breaks in the one kilometer fiber length, a helium neon laser was aligned and the beam was launched into the fiber end with no connector. An Amphenol connector was applied to the other end of the fiber and the laser light was visible coming out of the connector. Application of the ITT connector however, resulted in no visible or measurable optical power out of the connector. The reasons for this failure are believed to be related to the polishing stages of connector application. Examination of the connector end under a microscope reveals that the surface is not as highly polished as it should be. The conclusion reached was that connector application today is more of an art than a science. In order to become proficient one would need instruction, demonstration and practice.

The future of optical connectors is bright. Standards are being developed and imposed on manufacturers so that next generation devices will be smaller, more compatible and simpler to install. The proposal by Bell Telephone to lay a trans-oceanic fiber optic cable will spur research and development of a good underwater connector.

Because of the inability to install connectors, an off the shelf fiber optic system was used to demonstrate the modulation and demodulation schemes designed for the QUTR. The system, marketed by Spectronics, is called "The Missing Link" and comes with Siecor optical cable and installed Amphenol connectors.

The transmitter module, SPX 4140, comprises a complete functional optical transmitter for digital data. TTL compatibility allows direct connection to the encoding circuit described in Section C. The GaAlAs LED is integrated into a connector which is compatible with the Amphenol connectors attached to the fiber. Peak emission wavelength is 0.82 μm with maximum power out of .75 mW. This power decreases with fiber core diameter down to .07 mW into a 100 μm aperture. Data rates of up to 10 MHz are possible.

The SPX 4141 is the Spectronics receiver module matched to the SPX 4140 transmitter. The voltage out of the receiver is TTL compatible allowing direct connection to the demodulation circuitry described in Section G. The PIN diode

detector has a peak responsivity at 0.82 μm . The data format of the input is critical in that its short-term average must be constant. Pulse code modulation of a sinusoid satisfies this restraint.

Both the transmitter and receiver modules operate from a single +5 volt power supply. The supply, ground, and data pins were connected and the PCM signal was successfully transmitted over the Siecor fiber optic cable supplied (10 meters). The receiver was sensitive enough to be operated without applying an external bias voltage to the PIN diode. An increased cable length would require bias voltage on the PIN diode to increase its sensitivity.

F. OPTICAL RECEIVER

Optical detectors needed for fiber optic transmission systems must satisfy certain requirements regarding performance, compatability and cost. Important performance requirements are as follows:

1. High responsivity or sensitivity at the system operating wavelength.
2. Adequate bandwidth or speed of response to accommodate the data rate.
3. Minimum additional noise generated by the detector.
4. High reliability and low susceptibility of performance characteristics to encironmental conditions and changes.

Compatibility requirements for the QUTR application involve several considerations, although not as stringent as the optical transmitter which will be underwater. Physical size, fiber coupling and power supply requirements still need to be taken into account. Solid-state photodiodes satisfy most all requirements of performance, compatibility and cost. The two types of photodiodes which match the wavelengths of existing light sources are the avalanche photodiode (APD) and the PIN diode. The APD has an internal gain and therefore its responsivity is one to two orders of magnitude better than the PIN diode. The APD is about an order of magnitude more expensive than the PIN diode. In order to choose a detector, the smallest received signal must be matched to the smallest detectable signal without reducing the system bandwidth, or bit error rate. If a PIN diode would meet the specifications it would be the desired receiver over a APD.

The overall receiver transfer function can be defined by the ratio of output voltage to input current from the detector. The detector converts optical power into current and later stages of the receiver convert the current into voltage and then amplify it - usually to the same level as the voltage input to the transmitter (TTL). This transfer function is known as the transimpedance.

The receiver of a fiber optic system includes a low-noise front end amplifier optimized for use with the detector. Modules are commercially available which have detectors coupled to a preamplifier in a small, light-weight package. The detector current produces a voltage across a load resistor or feedback resistor. This voltage can be calculated by multiplying the received power, the responsivity and the effective load resistance.

The most important performance parameter for a digital communications system is bit error rate (BER). BER is the ratio of incorrect bits to total bits received. The BER decreases dramatically with small increases in optical power as the receiver SNR passes through the neighborhood of 20 dB [25]. For example, if a PCM system is operating at a BER of 10^{-8} , an increase in optical power of 1 dB will reduce the BER to 10^{-10} .

Using a Hewlett Packard PIN photodiode for a detector, a receiver circuit was designed and built. However, due to problems encountered with connector application mentioned earlier, this circuit was neither fully tested nor completely operational.

It is shown in Figure 24 only as a possible starting point in the construction of a receiver circuit and for signal power calculations in the following section. The HP-4220 is a low noise, high sensitivity, high speed PIN

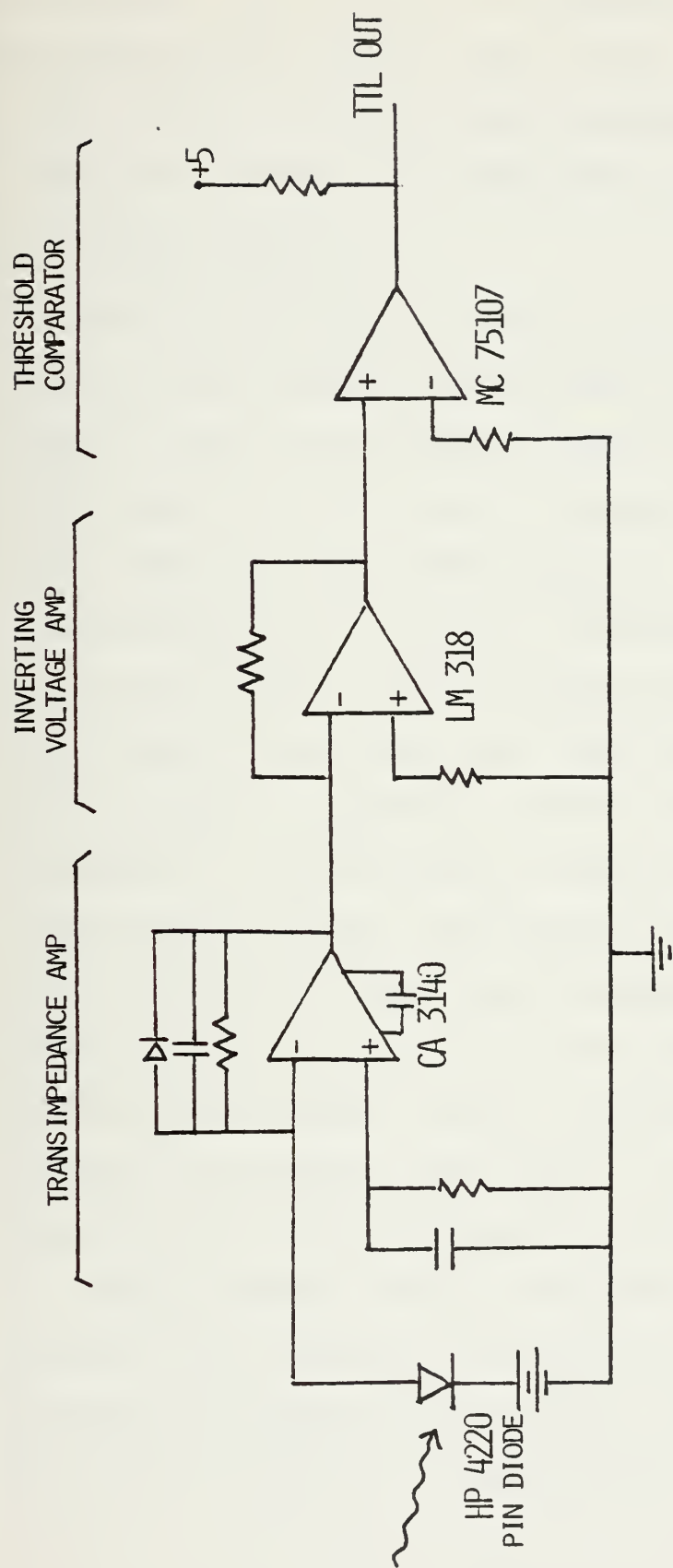


Figure 24 • Sample Receiver Circuit

photodiode. The CA 3140 is a PMOS/bipolar operational amplifier with a MOS/FET input stage. The MOS/FET input stage provides very high input impedance, very low input current and exceptional speed performance.

G. SIGNAL DEMODULATOR

Prior to discussing the demodulation scheme, a quick review of the overall system should be helpful to the reader. First, the torpedo traversing the shallow water range emits 1.5 μ sec bursts of energy in the form of acoustic waves every 12.5 μ sec (see Figure 2). These waves vary in frequency from 30 to 50 kHz. The hydrophones detect these signals and convert them to analog electrical voltage signals. These analog signals are then pulse code modulated, and a timing signal is inserted. The TTL voltage levels are then converted to current levels in order to on-off modulate a light emitting diode. The optical power out of the LED is then coupled into a fiber and transmitted to the beach (assuming the multiplexer is on the beach) where an optical detector and receiver convert the optical energy into current and then TTL voltage levels again. Now the PCM signal is present on the beach for further processing.

Recall from the earlier discussion of the signal format, that all the information transmitted is contained in the frequency components of the signal. The task at hand is to extract the frequency information from the PCM signal. One

obvious method would be to demodulate the PCM signal using a digital to analog converter and then measure the frequency of the reconstructed wave. This conversion would introduce additional error and although it is one alternative, a better alternative would be to somehow extract the frequency information directly from the PCM signal without a conversion to analog values. There is a simple method for accomplishing this which is ideally suited to a digital computer.

First, assume no noise is present. The received signal will be as illustrated in Figure 25. When the voltage value of the analog wave is greater than zero, the most significant bit (MSB) of the received signal is always high. When the analog signal falls below zero, the MSB is always zero. In other words, the MSB acts as a zero crossing detector. A square wave of the same frequency as the analog wave could be reconstructed using digital circuitry or the frequency itself could be computed through a simple software program if the data stream was input to the computer. The preferred method for the QUTR application would be through a computer for reasons to be discussed later.

A digital circuit was designed, built, and tested to demonstrate the capability of extracting the frequency component from the PCM signal. Looking at Figure 26, the PCM signal is fed to a decoder acting as a one to eight

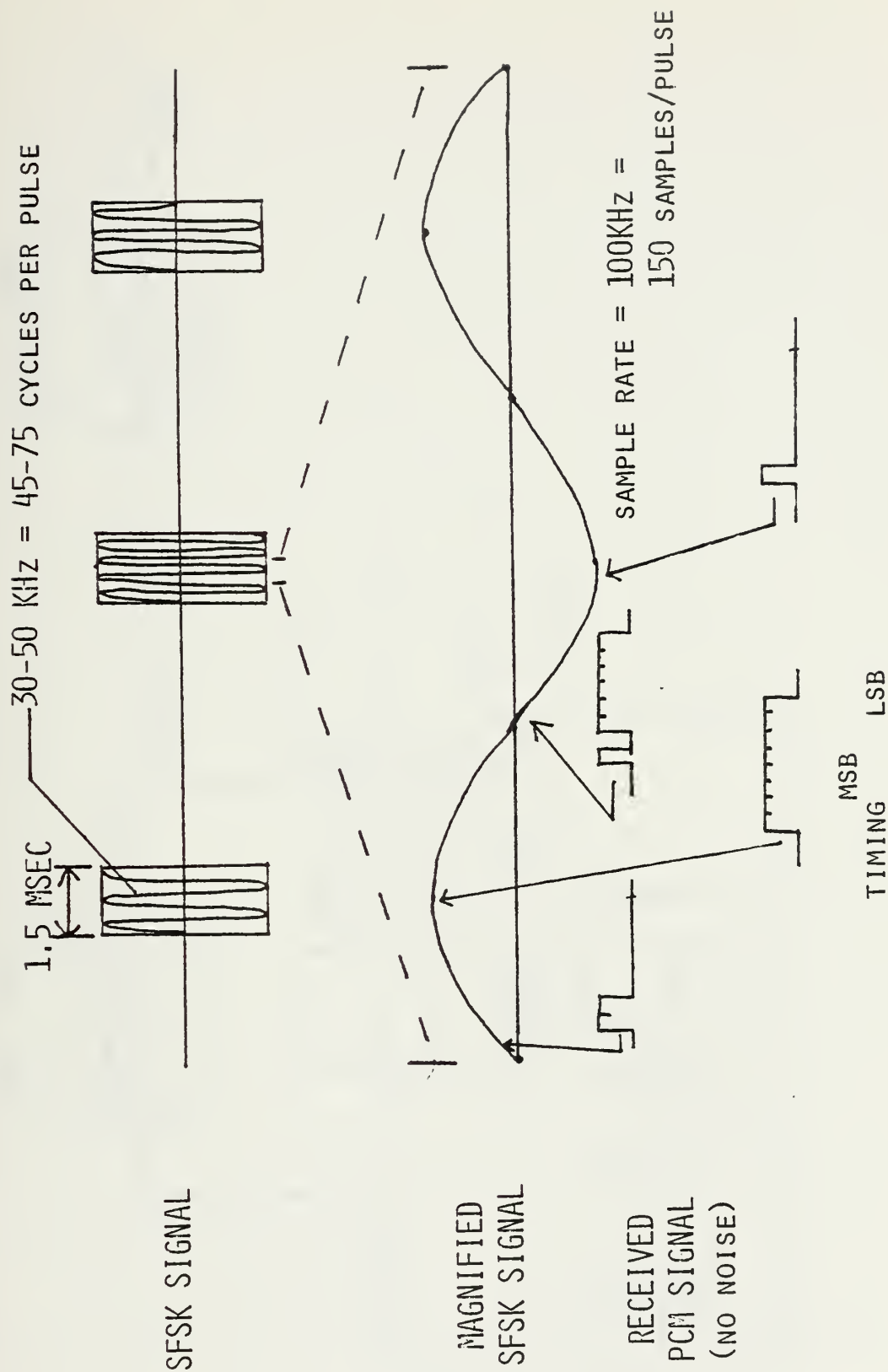


Figure 25. Signal Conversion From Analog SFSK to Digital PCM

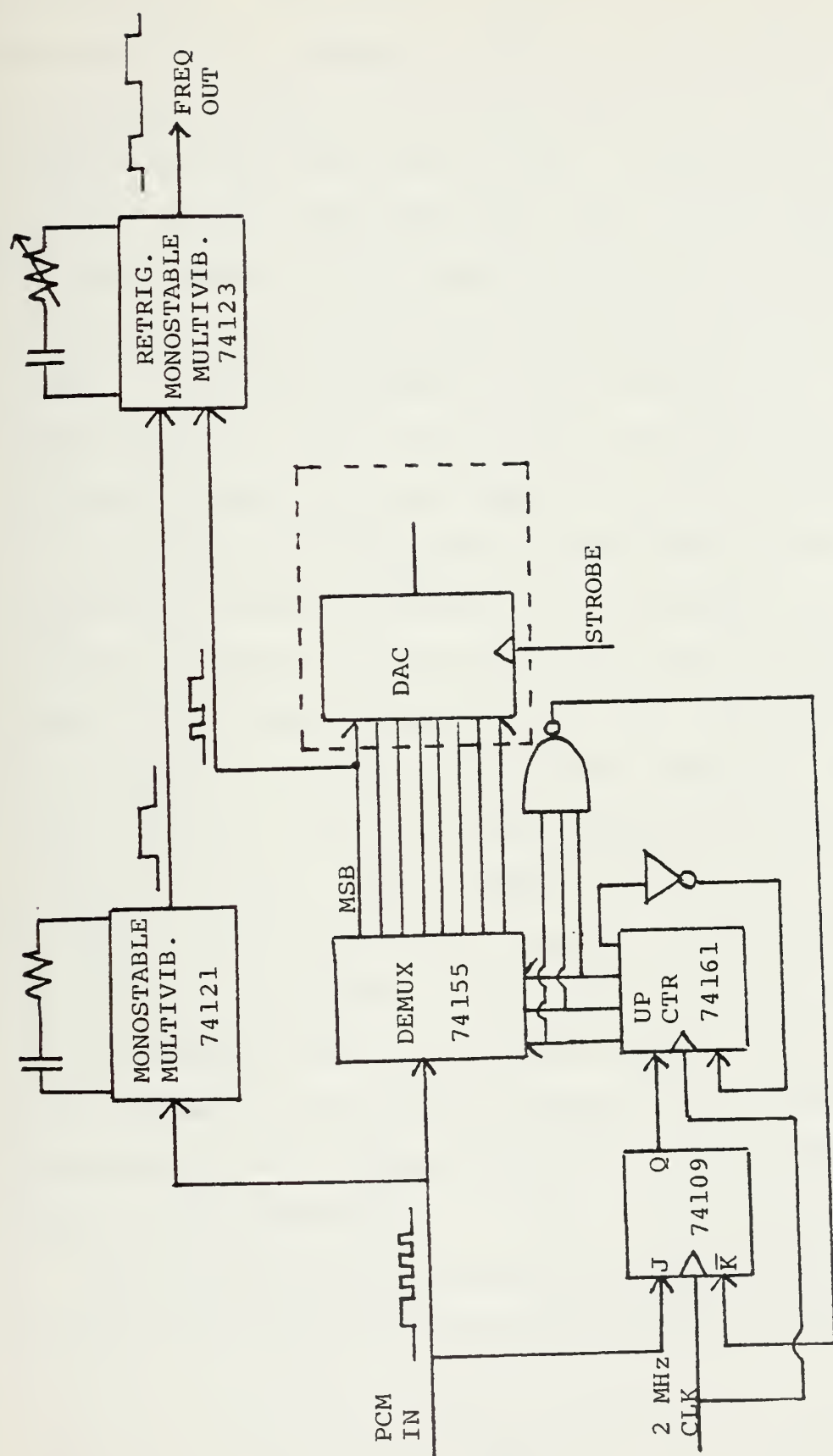


Figure 26. Block Diagram of Demodulator

demultiplexer. The signal is also fed to a J-K flip-flop. The first bit or timing bit turns on the flip-flop which activates a counter. The counter will allow the decoder to demultiplex the seven bits of data. Feeding the counter outputs through a NAND gate back into the flip-flop turns off the counter until the next timing bit is received. The clock required for circuit operation must be set on or close to the clock frequency of the transmitter. This frequency is not real critical since the clock, in effect, is synchronized after every eight bits by the timing pulse.

The more interesting part of the circuit is the section containing the multivibrators. The monostable multivibrator (74121) generates a .4 μ sec pulse for every timing bit as shown in the timing diagram (Figure 27). The MSB out of the decoder is inverted and logically ANDed with the .4 μ sec pulse from the 74121 in the retriggerable monostable multivibrator (74123). When the $\overline{\text{MSB}}$ is low and the 74121 output is high, a pulse is produced slightly longer than 10 μ sec. Now if two or more MSB's in a row are high, the multivibrator will retrigger until a low MSB is received. It will then stay low until a high MSB is received. The result is a square wave whose average frequency is that of the analog wave at the hydrophone.

Due to the lack of a constant frequency square wave at the output, the use of an oscilloscope to observe the

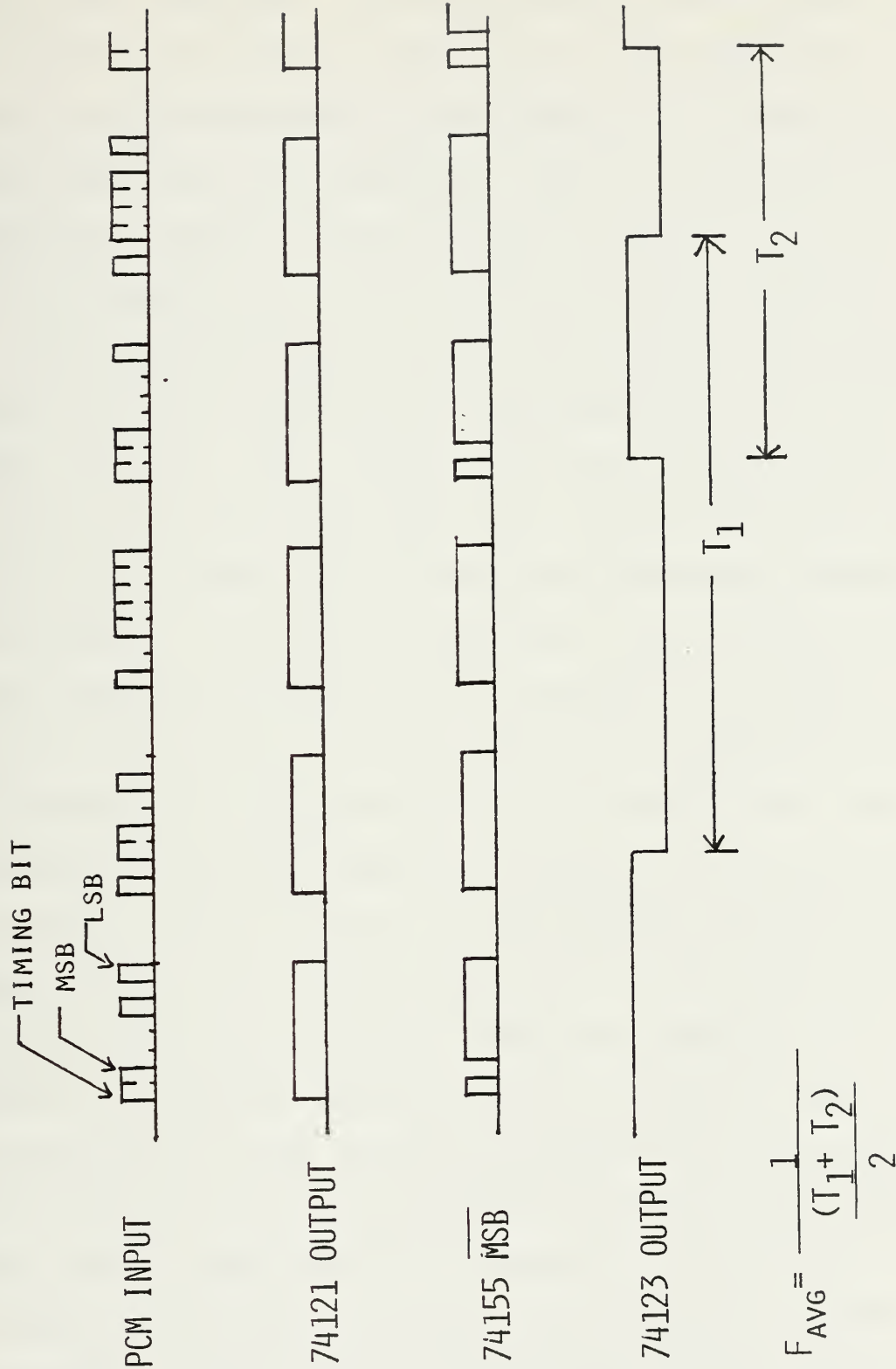


Figure 27. Demodulator Circuit Timing Diagram

output was impossible. The scope would never trigger and presented only a blur on the screen. With a HP 5302A frequency counter connected to the output, the frequencies and their variations were observed. Good correlation with the frequency transmitted was obtained as long as the transmitted frequency was under 50 kHz, the Nyquist frequency.

Since only the MSB is used in this circuit, the question arises as to the value of the remaining six bits of each eight bit word. When the sampling rate is only slightly greater than the Nyquist rate, very little information is contained in those bits as far as the frequency component is concerned. As noise is introduced, the probability of error markedly increases. We are making our decision on only one bit out of each eight bit word. As the sampling rate is increased to much greater than the Nyquist rate, the frequency information begins to spread out into the other six bits. A good fraction of the frequency information is still in the MSB but now we can also use the other bits to help in the extraction of the frequency component of the signal. A computer program could be written to check all the bits in the noisy signal and compare them with prior words and future words to determine the most likely signal sent. As the sampling rate is increased from 100 kHz, this method will give more accuracy at the expense of signal bandwidth. As will be seen in the next section, the optical

channel is not close to being bandwidth limited. Although the analog to digital converter in the PCM modulator is limited to a sample rate of 250 kHz, there are other converters that can give an order of magnitude faster sample rates.

H. SIGNAL POWER BUDGET AND DISPERSION CALCULATIONS

While optical fibers offer lower losses of signal power than do coaxial cables, some attenuation does exist. In addition, some loss of signal power occurs wherever a connection is made, whether it be a source-fiber connector, fiber-detector connector, or fiber-fiber connector. Power losses in a connector are caused by core diameter mismatch, core numerical aperture mismatch, fiber gap separation, axial misalignment of fibers, angular misalignment of fibers, and Fresnel reflection at interfaces.

Signal power loss calculations enable the designer to plot a loss budget analysis and predict the performance of a fiber optic communication system. For the proposed system, a link power budget was made for both the standard wavelength of 0.82 μm and the higher wavelengths. Optical losses associated with the various system components can be clearly seen in Figure 28 and opportunities for improvement or limitations identified.

First, the minimum optical power required by the receiver must be determined. This value may be given as the noise

equivalent power (NEP) which is the radiant flux necessary to give an output signal equal to the detector noise. Another way to determine minimum detectable power is by deriving an expression for signal to noise ratio at the amplifier output, set that value equal to one and solve for the power as follows:

$$\frac{S}{N} = \frac{\overline{i_s^2}}{\overline{i_{N1}^2} + \overline{i_{N2}^2}} \quad (7)$$

where $\overline{i_s^2}$ is the mean square signal current, $\overline{i_{N1}^2}$ is the mean square shot noise current, and $\overline{i_{N2}^2}$ is the mean square thermal noise (Johnson).

Shot noise is caused by the random fluctuations in the rate of arrival of the electrons at the collecting electrode. Shot noise is represented by:

$$\overline{i_{N1}^2} = 2eI_{dc}\Delta f \quad (8)$$

where e is the charge of the electron, I_{dc} is the average DC current, and Δf is the signal bandwidth.

Thermal noise is white noise occurring in all conducting materials. It is a consequence of the random motion of electrons through a conductor. Thermal noise is given by:

$$\overline{i_{N2}^2} = \frac{4kT_e\Delta f}{R_L} \quad (9)$$

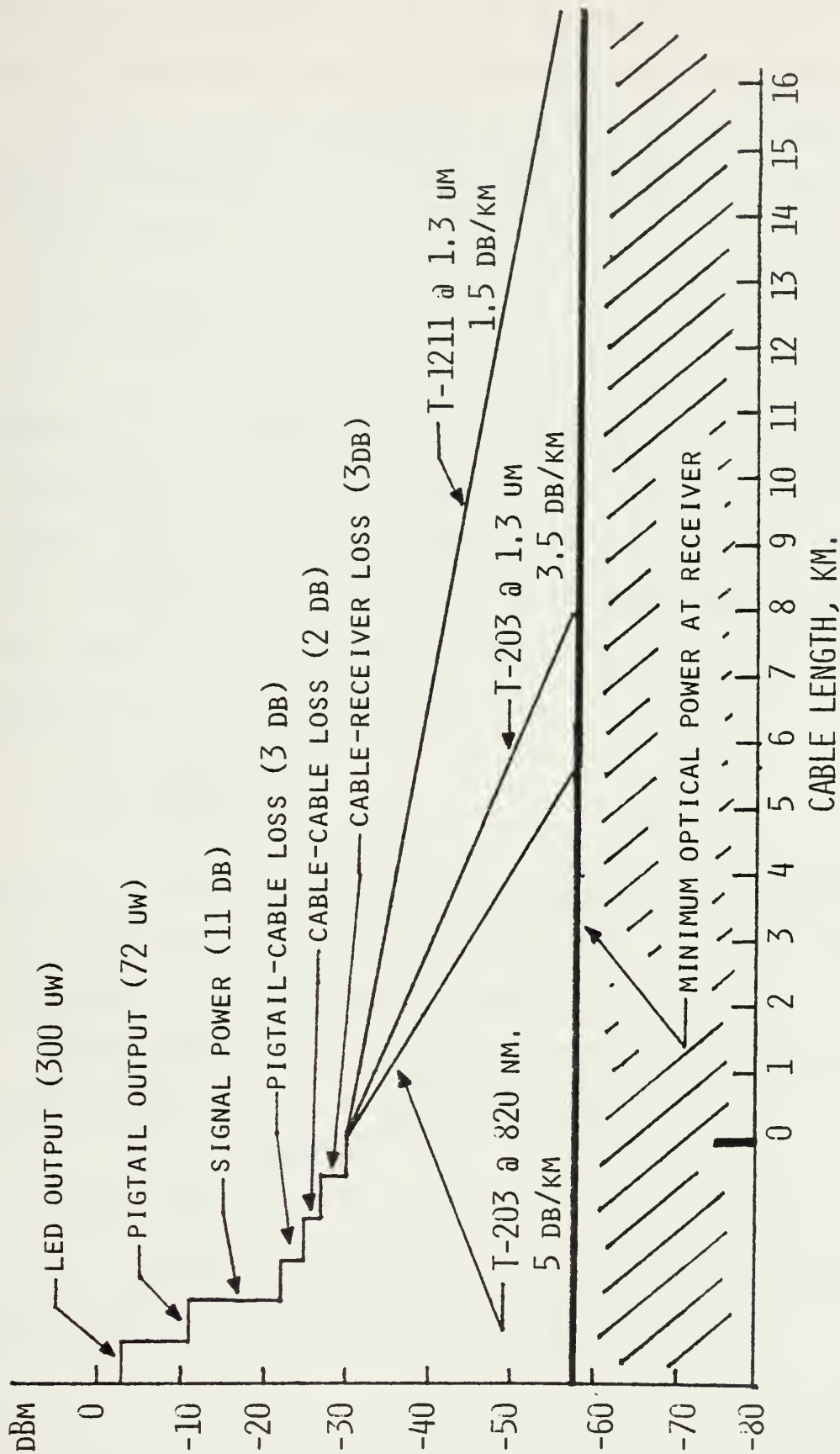


Figure 28. Optical Power Budget

where k is Boltzmann's constant, T_e is the effective input noise temperature and R_L is the diode load resistance.

In order for the photodiode to have a fast enough response time to accommodate the modulation frequency of the light, R_L must be kept at a small value since:

$$\omega_m \ll \frac{1}{R_L C_d} \quad (10)$$

where ω_m is the modulating frequency and C_d is the diode capacitance [25]. With R_L small, the value of i_{N2}^2 becomes large. This noise term becomes dominant over the shot noise term. Therefore, the detector is thermal noise limited and shot noise can be ignored. Under these assumptions the signal to noise ratio becomes:

$$SNR = \frac{2(P_e \eta / h\nu)^2}{4kT_3 \Delta\nu / R_L} \quad (11)$$

where P is the signal power, η is the detector efficiency, ν is the light frequency given by $\nu = C/\lambda$, $\Delta\nu$ is the signal bandwidth and h is Planck's constant.

Setting SNR to one and solving for P gives the desired expression for minimum detectable power:

$$P_{min} = \frac{h\nu}{e\eta} \sqrt{\frac{2kT_e \Delta\nu}{R_L}} \quad (12)$$

Since in practice, R_L is related to the signal bandwidth and the junction capacitance C_d by [25],

$$\Delta v \approx \frac{1}{2\pi R_L C_d} , \quad (13)$$

this expression can be substituted into Equation (11) to give:

$$P_{\min} \approx 2\sqrt{\pi} \frac{h\nu\Delta v}{e\eta} \sqrt{kT_e C_d} \quad (14)$$

where $h = 6.6 \times 10^{-34}$ watt sec²

$$\nu = c/\lambda = 3 \times 10^8 / .820 \times 10^{-6} = 3.66 \times 10^{14} \text{ sec}^{-1}$$

$$\Delta v = 2/\pi\tau = 1.27 \times 10^6 \text{ sec}^{-1}, = \text{PCM bit period}$$

$$e = 1.6 \times 10^{-19} \text{ joule}$$

$$\eta = .7, \text{ from HP 4220 specifications}$$

$$k = 1.38 \times 10^{-23} \text{ watt sec } ^\circ\text{K}^{-1}$$

$$T_e = T_d + (F-1) \times 290, \text{ assuming a noise figure of 6dB and diode temperature of } 290 ^\circ\text{K}$$

$$T_e = 290 + (4-1) \times 290 = 1160 ^\circ\text{K}$$

$$C_d = 1.5 \times 10^{-12} \text{ farads, from HP 4220 specifications.}$$

So:

$$P_{\min} = 1.5 \times 10^{-9} \text{ watts or } -58\text{dBmW} \quad (15)$$

Now that the minimum detectable signal is known, the signal to noise ratio required for a certain bit error rate (BER) must be determined. Earlier it was mentioned that as receiver SNR passes through the neighborhood of 20 dB the BER decreases dramatically. Using the standard assumption that the noise is Gaussian, the probability of error curves

for binary pulse trains may be used to determine that for a BER of 10^{-9} the current SNR must be [35]:

$$\frac{i_s}{\langle i_N \rangle} = 11.9 \text{ (21.5dB)} \quad (16)$$

Converting this to power gives about 11dB shown on the power budget graph (Figure 28) as signal power. The LED output of 300 μ watts is from the IRE 160 FB specifications and the power out of the fiber pigtail was measured as 72 μ watts. The connector losses of 3dB for fiber to device and 2dB for fiber to fiber are maximum losses for current technology. Future connectors will improve upon these figures. Using T-203 fiber at .82 μ m the losses are 5dB/km. For comparison the plot for T-203 fiber at 1.3 μ m and another ITT fiber T-1211 at 1.3 μ m is shown in Figure 28. Using T-203 fiber would not allow signal transmission at the desired BER for the required 16 kilometers. Several alternatives are available:

1. Use a higher power LED. These are, in fact, available in the 1 mw area for various wavelengths.
2. Increase the maximum acceptable BER. This would help very little since large changes in BER in this area give only small changes in SNR.
3. Use of different fiber with lower attenuation. This solution will give by far the largest improvement. Shown in Figure 28, is the T-1221 fiber, with a 1.5 dB/km attenuation at 1.25 μ m.

Using a T-1211, a fiber link could be run from a hydrophone to the beach with no repeaters involved. A connector fitting where the multiplexer is now planned could connect each individual hydrophone fiber into one multi-fiber cable to the beach.

Rise time is a valuable measure of a fiber's dispersive properties. It is used in a system design analysis to ensure that the components selected operate at the required speed. System rise time must be calculated in order to determine if the signal dispersion is a bandwidth limiting factor. Since the dispersion decreases as wavelength increases up to about 1.3 μm , if an acceptable value is obtained for 820 nm, the value for 1.3 μm will be even better. For 2 MBPS the maximum required rise time is 350 nsec which is much greater than the system rise time of 86 nsec as shown in Table 2 [6].

Light Source: IRE 160 FB	<u>Rise Time</u>
$\lambda = 820 \text{ nm}$	$t_1 = 14 \text{ ns}$
$\Delta\lambda = 40 \text{ nm}$	
Photodetector: HP 4220	$t_2 = 1 \text{ ns}$
-20 v bias	
Modal Dispersion: T 203 fiber	$t_3 = 56 \text{ ns}$
3.5 ns/km x 16 km	
Material Diapersion	$t_4 = 52 \text{ ns}$
$16 \text{ km} \times 820 \times 10^{-9} \times 40 \times 10^{-4}$	
System Rise Time = $1.11\sqrt{t_1^2 + t_2^2 + t_3^2 + t_4^2} =$	86 ns
Total Allowable Rise Time for 2 MBPS Digital NRZ	$= 0.7/2 \text{ } \mu\text{s}$
	$= 350 \text{ ns}$

Table 2. Rise Time Calculation

III. CONCLUSIONS AND RECOMMENDATIONS

Fiber optic technology has been progressing at such a rapid rate that a noticeable advancement in several areas has taken place just since the outset of this work. Increased attention has been directed towards standardization - one of the biggest problems. In April 1978, the Electronic Industries Association formed a committee with the intent and purpose of standardizing the fiber optic area. Now, the Department of Defense has allocated a Federal Stock Group in their supply system for fiber optics. Federal Stock Group 60 is divided as follows:

- 6010 Fiber Optic Conductors
- 6015 Fiber Optic Cables
- 6020 Fiber Optic Cable Assemblies
- 6030 Fiber Optic Devices
- 6070 Fiber Optic Accessories
- 6080 Fiber Optic Kits

This step by the Defense Supply System should contribute to standardization among military users.

Operating wavelengths greater than one micrometer are fast gaining in popularity. The British Post Office has recently tested a 1.3 micrometer receiver using a GaInAs PIN photodiode and an FET amplifier. At 140 MBPS the mean

received optical power was -44 dBm at a BER of 10^{-9} . In Long Beach, Bell Telephone has installed a link operating at the longer wavelength. Incorporation of longer wavelength sources and detectors into the QUTR could allow repeaterless links of up to 20 kilometers with current technology.

Emphasis on simplicity in a fiber optic link seems to be increasing. A direct result of longer wavelength operation is circuit simplicity in the transmitter and receiver. Some systems no longer need the power of a laser source or sensitivity of an avalanche photodiode. This means the simpler circuitry associated with LED's and PIN diodes can be employed. A concentrated effort in simple cable termination must also be made.

Longer wavelengths prove advantageous in the quest for having less electronics underwater in the QUTR application. A fiber link from each hydrophone directly to the beach is now feasible with regard to attenuation. One possibility would be to have an "octopus" type fitting where the multiplexer is now planned. Individual cables from each hydrophone could be connected to one fiber of a multi-fiber cable running to the beach. For 16 hydrophones a 16 fiber cable would be required. By coupling power into 16 fibers instead of one, the bandwidth is improved by 16 since the receiver noise goes up linearly with receiver bandwidth. Also, since the power is increased 16 times at the receiver, a longer transmission distance at the same bandwidth is achieved.

Pulse code modulation offers a flexible and efficient means of achieving improved noise performance with bandwidth expansion and is particularly attractive for fiber optic systems. Because of the bandwidth capability of optical fibers, the bandwidth expansion caused by the binary representation of analog information tends not to be the disadvantage that it often is with strictly band-limited channels. Because the Doppler shifted carrier wave is being digitized, the Doppler information is contained in the digital signal. This information could be used in torpedo velocity determinations and potentially help in the tracking algorithm.

All the signal information can be extracted from the PCM digital pulse stream without converting back to an analog waveform. As the PCM sample rate is increased, the bits other than the most significant bit become more important. Because noise is introduced into the system, a linear interpolation algorithm becomes beneficial. If a bit is in error, the computer program looks at the preceding word and the next word and then interpolates between the two. This computer "guessing" of the correct bit works best on smooth waveforms which is the case with SFSK.

The future of fiber optic systems is bright. Current trends and developments have been discussed and related to the QUTR. A range layout and data format have been suggested

and shown to be performable. Although individual component costs were mentioned and compared, an overall cost analysis was not undertaken. The best system is the cheapest system that will do the job. It has been shown that relatively cheap sources can be used if a higher quality fiber is employed. In general, the price of the optical sources should be kept down since there may be up to 16 of them. The costs and tradeoffs of moving the multiplexer to the beach need yet to be studied. Once the costs have been determined favorable to a fiber optics system for the QUTR, total system acceptance will be a function of component maturity and management commitment. It can be concluded from this work, that component maturity is no longer a limitation.

LIST OF REFERENCES

1. Forrest M. Mims, III, "Alexander Graham Bell and the Photophone: The Centennial of the Invention of Light-Wave Communications, 1880-1980", Optics News, Vol. 6, No. 1, pp. 8-15.
2. John R. McHenry, Fiber Optic Design Application for a Shallow Water Torpedo Tracking Range, MSEE Thesis, Naval Postgraduate School, Monterey, CA, March 1979.
3. David N. Nicholson, Fiber Optic Link Design for an Open Ocean Shallow-Water Tracking Range, MSEE Thesis, Naval Postgraduate School, Monterey, CA, March 1980.
4. H. F. Taylor, Transfer of Information on Naval Vessels via Fiber Optics Transmission Lines, San Diego, CA, Naval Electronics Laboratory Center, May 1971.
5. Michael K. Barnoski, Fundamentals of Optical Fiber Communications, New York, New York, Academic Press, Inc., 1976.
6. Glenn R. Elion, Herbert A. Elion, Fiber Optics in Communication Systems, New York, Marcel Dekker, Inc., 1978.
7. John E. Midwinter, Optical Fibers for Transmission, New York, John Wiley & Sons, 1979.
8. Dan Botez, Gerald J. Herskowitz, "Components for Optical Communications Systems", Proceedings of the IEEE, Vol 68, No. 6, pp. 689-718, June 1980.
9. Harvey J. Hindin, "Bell Installs Long-Wavelength Fiber System", Electronics, Vol. 53, No. 15, pp. 59, July 3, 1980.
10. Kenneth Dreyfack, "Fiber Optic Net to Link Thousands of Homes", Electronics, Vol. 53, No. 16, pp. 81-82, July 17, 1980.
11. L. C. Gunderson, "Future Developments for Fiber Optics", presented at the International Conference on Fibre Optics in Industry, London, England, March 21, 1980.
12. Michael Wenyon, "Europe Tests Broadband Systems", Laser Focus, Vol. 16, No. 7, pp. 56-60, July 1980.

13. T. P. Lee, J. C. Campbell, A. G. Dentai, C. A. Burrus, "Dual-Wavelength Demultiplexing InGaAsP/InP Photodiode", in 1979 Optical Fiber Communications, 1979, pp. 92-94.
14. K. Kobayashi, M. Seki, "Micro-Optic Grating Multiplexers for Fiber Optic Communications", in 1979 Optical Fiber Communications, 1979, pp. 54-56.
15. Mituso Kajitani, Kazumasa Tsukada, Shigeo Aoki, "Single-Fiber Bidirectional Data Bus Loop With Sixty Data Bus Couplers", in Conference on Laser and Electro-Optical Systems, Feb. 1980, pp. 34.
16. K. Minemura, K. Kobayashi, H. Nomura, S. Matsushita, A. Ueki, "Two-Channel 400 Mbit/sec 36 Km. WDM Transmission Experiments in the 1 μ m Band Using Single-Mode Fibers", in Conference on Laser and Electro-Optical Systems, Feb. 1980, pp. 40-42.
17. J. Conradi, J. Straus, A. J. Springthorpe, J. C. Dymont, R. Maciejko, G. Duck, W. Sinclair, I. Few, P. Devlin, "Wavelength Division Multiplexed Multichannel Video Transmission System", in Conference on Laser and Electro-Optical Systems, Feb. 1980, pp. 42-43.
18. J. A. Bucaro, "Optical Fiber Sensors", in Conference on Laser and Electro-Optical Systems, Feb. 1980, pp. 64-65.
19. J. N. Fields, C. P. Smith, C. K. Asawa, R. J. Morrison, O. G. Ramer, G. L. Tangonan, M. K. Barnoski, "Multimode Optical-Fiber Loss-Modulation Acoustic Sensor", in 1979 Optical Fiber Communications, 1979, pp. 58-59.
20. Dixon R. Doll, Data Communications, New York, John Wiley & Sons, 1978.
21. R. L. Gallawa, A Users Manual For Optical Fiber Communications, Springfield, VA, NTIS, 1976.
22. NAVSHIPS 0967-291-6010, Principles of Modems, Washington, D.C., GPO, 1978.
23. Donald C. O'Shea, W. Russell Callen, William T. Rhodes, Introduction to Lasers and Their Applications, Reading, MA, Addison-Wesley Publishing Company, 1978.
24. D. Gloge, "Second Generation Fiber Systems", Optical Spectra, Vol. 13, Issue II, pp. 50-52, Nov. 1979.

25. Amnon Yariv, Introduction To Optical Electronics, San Francisco, CA, Holt, Rinehart and Winston, Chap. 11, 1976.

INITIAL DISTRIBUTION LIST

	No. Copies
1. Defense Technical Information Center Cameron Station Alexandria, Virginia 22314	2
2. Library, Code 0142 Naval Postgraduate School Monterey, California 93940	2
3. Department Chairman, Code 62 Department of Electrical Engineering Naval Postgraduate School Monterey, California 93940	1
4. Professor John Powers, Code 62Po Department of Electrical Engineering Naval Postgraduate School Monterey, California 93940	5
5. Professor Glen Myers, Code 62Mv Department of Electrical Engineering Naval Postgraduate School Monterey, California 93940	1
6. Professor O. B. Wilson, Code 61W1 Department of Physics Naval Postgraduate School Monterey, California 93940	1
7. Mr. R. L. Marimon, Code 70 Naval Undersea Warfare Engineering Station Keyport, Washington 98345	1
8. Commander C. Gertner, Code 80 Naval Undersea Warfare Engineering Station Keyport, Washington 98345	1
9. Mr. R. L. Mash, Code 50 Naval Undersea Warfare Engineering Station Keyport, Washington 98345	1
10. Mr. Richard Peel, Code 7021 Naval Undersea Warfare Engineering Station Keyport, Washington 98345	3
11. Lieutenant David A. Andersen 1845 Harvard Avenue Gretna, Louisiana 70053	2

- | | | |
|-----|--|---|
| 12. | Administrative Department, Code 0115
Naval Undersea Warfare Engineering Station
Keyport, Washington 98345 | 5 |
| 13. | Professor R. Panholzer, Code 62Pz
Department of Electrical Engineering
Naval Postgraduate School
Monterey, California 93940 | 1 |
| 14. | Captain David N. Nicholson
SAFSP-5
P. O. Box 92960, Worldway Postal Center
Los Angeles, California 90009 | 1 |
| 15. | Commandant (G-PTE-1/72)
U. S. Coast Guard
Washington, D.C. 20593 | 2 |

Thesis

190767

A4425 Andersen

c.1

A pulse code modulated fiber optic link design for quinault

under-water tracking range.
12 AUG 1970

Thesis

190767

A4425 Andersen

c.1

A pulse code modulated fiber optic link design for quinault under-water tracking range.

thesA44425

A pulse code modulated fiber optic link



3 2768 000 99125 1

DUDLEY KNOX LIBRARY